ANNUAL REVIEWS

Annual Review of Control, Robotics, and Autonomous Systems

Stimuli-Responsive Polymers for Soft Robotics

Yusen Zhao,[1] Mutian Hua,[1] Yichen Yan,[1] Shuwang Wu,[1] Yousif Alsaid,[1] and Ximin He[1,2]

[1]Department of Materials Science and Engineering, University of California, Los Angeles, California, USA; email: ximinhe@ucla.edu

[2]California Nanosystems Institute, Los Angeles, California, USA

Annu. Rev. Control Robot. Auton. Syst. 2022. 5:515–45

First published as a Review in Advance on November 17, 2021

The *Annual Review of Control, Robotics, and Autonomous Systems* is online at control.annualreviews.org

https://doi.org/10.1146/annurev-control-042920-014327

Keywords

liquid crystal polymers, hydrogels, shape memory polymers, magnetic elastomers, electroactive polymers, thermal expansion actuators

Abstract

This article reviews recent progress in the use of stimuli-responsive polymers for soft robotics. First, we introduce different types of representative stimuli-responsive polymers, which include liquid crystal polymers and elastomers, hydrogels, shape memory polymers, magnetic elastomers, electroactive polymers, and thermal expansion actuators. We focus on the mechanisms of actuation and the evaluation of performance and discuss strategies for improvements. We then present examples of soft robotic applications based on stimuli-responsive polymers for bending, grasping, walking, swimming, flying, and sensing control. Finally, we discuss current opportunities and challenges of stimuli-responsive soft robots for future study.

1. INTRODUCTION TO SOFT ROBOTICS

Soft robotics has emerged as a research field that is pushing the boundaries of conventional robots. Numerous notable achievements have been made recently, including a granular jamming gripper (1), continuum fiber robot (2), worm robot (3, 4), jumping robot, integrated octobot (5), self-oscillating swimmer (6), and flying robot (7), among many others. The use of soft matter with a low Young's modulus allows for mechanical compliance and continuous deformability in robots; soft matter can easily conform to the surfaces of objects and adapt to unstructured environments (8, 9). Such soft systems are particularly important for wearable devices, drug delivery (10), surgery (11), and rehabilitation (12, 13).

Several key features merit consideration for a soft system that can be used practically, including the produced force, deformation strain, response rate, energy density, function, scaling, auxiliary equipment, and reliability. However, trade-offs among these parameters usually exist, and researchers are expected to balance them in specific working scenarios. It is highly desirable to achieve enhanced performance without sacrificing other characteristics. In addition, researchers can take inspiration from biological systems for the actuation principle and develop novel actuation functionalities through biomimicry (14). To accomplish more advanced robotic locomotion with autonomy, a highly compact system that incorporates a sensory–actuation feedback loop with minimal manual control is desirable, creating a soft robot with proprioception (self-perception). Other challenges for future soft robot design include reducing robot tethering; utilizing onboard battery or remote power; and developing actuator, sensing, control, and other regulation strategies (8, 15).

Studies of soft actuation incorporate working mechanisms, material designs, and control systems to enable completely soft and functional robots. The working mechanism of actuation is closely related to the material selection while also determining the performance and potential applications. Although soft actuators can be made using stiff materials through geometrical designs in the form of mesh, foam, springs, and wires, this review does not focus on these types of actuators, because of their limited strain and fewer degrees of freedom for complex functionalities (3, 16). For intrinsically soft actuators, pneumatic actuators and hydraulic actuators have been regarded as effective choices in the past decade, because of their relatively high delivered force, fast response time, large deformation strain, and design customizability. The materials for these types of robots are mainly silicone elastomers due to their facile fabrication, mechanical robustness, and low elastic hysteresis. Engineering the material with microscale geometry can enable the actuator to deform in prescribed ways, such as expansion (17), asymmetric bending motion (18), and rotation (19). Many works have already been established in conjunction with pneumatic and hydraulic actuators to integrate more advanced functions and perform complex tasks, such as proprioceptive sensing (20) and closed-loop control (21). However, they suffer from the fact that they require tethered tubing to provide air or fluid inflation, auxiliary equipment, and predefined actuation. To tackle these problems, a few examples of untethered pneumatic actuators have been reported, based on the evaporation of a solvent with a low boiling point (22) and the production of gas from chemical reactions (5, 23). In addition, many challenges remain to be addressed to realize miniaturized untethered soft robots, which require scale-down while carrying components such as batteries, electronic controller, motors, and pumps onboard.

Bio-hybrid actuation presents another emerging research direction using biological materials (such as muscle tissue) as actuators to achieve softness and biocompatibility. The actuation can be powered by either an electric field or light. For example, a jellyfish robot created by combining elastomers and dissociated rat tissue is capable of self-propulsion underwater in the presence of an electric field (24). A stingray robot composed of cardiomyocytes can achieve phototactic swimming and can be navigated by light to bypass obstacles (25). Although promising, the field

is still in a nascent state and requires further improvements to material properties, environmental compatibility, and the necessity to keep cells or tissue alive.

2. STIMULI-RESPONSIVE POLYMERS FOR ACTUATORS AND SOFT ROBOTS

Stimuli-responsive polymers are an area of soft robotics that is undergoing rapid innovation. These materials can change their chemical and physical properties in response to external stimuli, including heat (26), light (27), pH (28), humidity (29), magnetic fields (30), and electric fields (31). Tremendous research has focused on improving characteristics without sacrificing performance in different smart materials, including liquid crystal (LC) materials, hydrogels, shape memory polymers (SMPs), electroactive polymers (EAPs), magnetic polymers, and thermal expansion actuators (**Figure 1**).

One advantage of stimuli-responsive polymers is that the actuation performance and robotic locomotion are determined largely by the molecular modulation and chemical modification of the smart polymers. Demonstrating uniquely tunable performance, stimuli-responsive polymers are promising as artificial muscles, grippers, locomotive robots, swimming robots, and even flying robots. In addition, the stimulus can be customized when designing robots for different demands. For example, an electrical stimulus is advantageous when fabricating a highly compact system with accurate control but usually requires tethered electrical connections for power and computation. Smart polymers stimulated by heat, light, and magnetic fields can be operated in an untethered pathway, a design that greatly improves miniaturization since the robot is fueled through external stimuli rather than onboard equipment. Magnetic fields can penetrate through materials and most biological tissues, but bulky external instruments limit their use in open areas. **Table 1** lists several stimuli-responsive polymers actuated by different stimuli.

The intrinsic multifunctionality of stimuli-responsive polymers has expanded the scope of soft robots to potentially replace some rigid robots or traditional soft robots; this article reviews recent advances in stimuli-responsive polymers for actuators and provides some insights into designing smart soft robots. First, we describe different types of representative stimuli-responsive polymers and evaluate their potential for soft robotics. Then, we discuss applications and opportunities of these materials in soft robotics. Finally, we consider the current challenges in the use of stimuli-responsive materials for robotic applications and provide our perspectives.

2.1. Liquid Crystal Elastomers and Networks

LC is a state of matter that has positional and/or orientational organization in its molecular arrangement. Liquid crystal polymers (LCPs), liquid crystal elastomers (LCEs), and liquid crystal polymer networks (LCNs) have been studied as promising materials that can change shape in response to external stimuli. The differences among these materials—namely, their chemical compositions, cross-linking, and thermomechanical properties—are shown in **Figure 2*a***. In this section, we focus mainly on LCEs that respond to temperature, light, and electric fields.

2.1.1. Thermally responsive liquid crystal elastomers. Under heating, the LC moieties undergo a transition from an anisotropic phase to an isotropic phase, which changes the system from an ordered state to a disordered state. The structural unit of LC materials is a tightly packed rod-like mesogen. In the case of typically uniaxially aligned LC materials, the average spacing of mesogens is reduced along the oriented direction and increased in the perpendicular direction. As a result, the material contracts along the oriented direction and expands in the perpendicular direction (**Figure 2*b***). Specifically, LCPs with a main-chained non-cross-linked polymer have a low

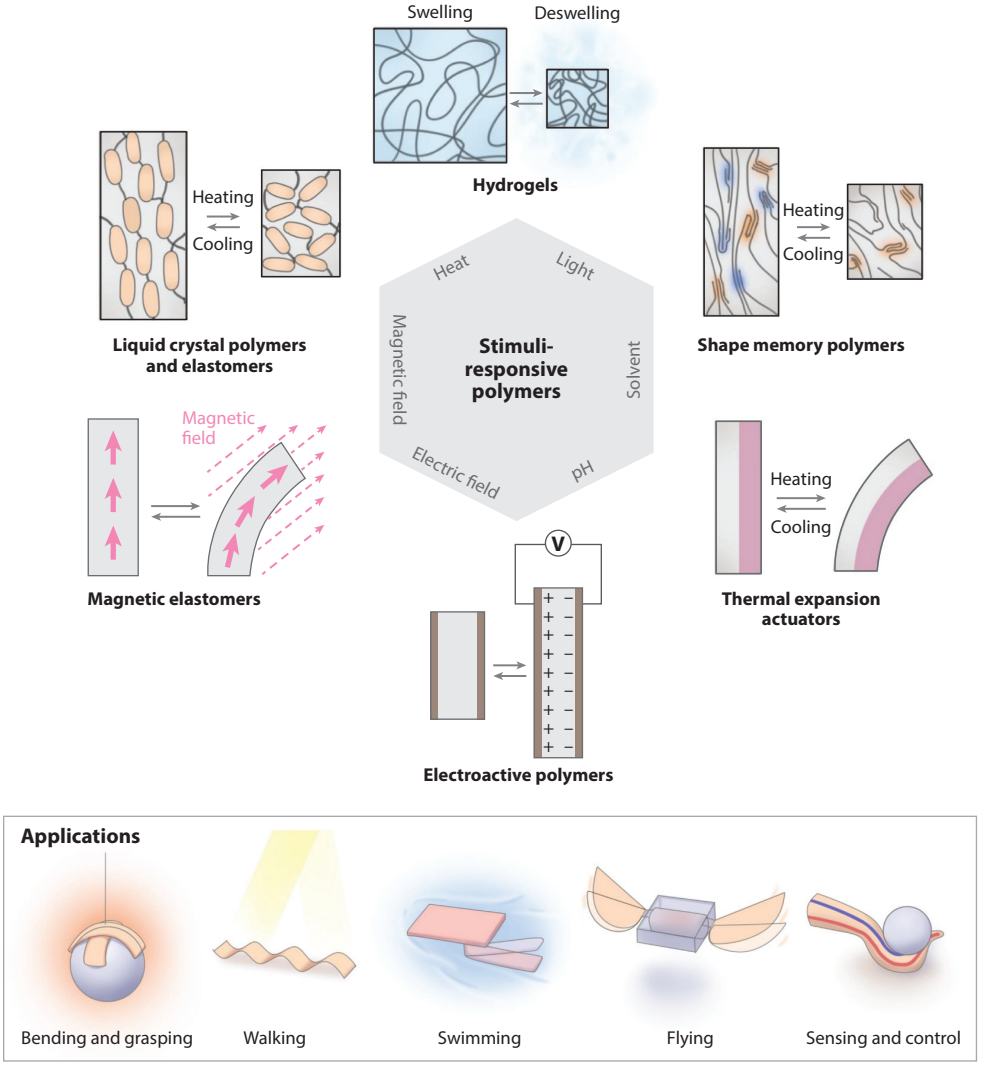

Figure 1

Stimuli-responsive polymers and applications in soft robotics.

actuation ratio. LCNs with a moderate to densely cross-linked network and a glass transition temperature above room temperature usually have a molecular ordering change of <5%. By contrast, LCEs that contain a variety of flexible chains and have a glass transition temperature below room temperature can largely deform (by more than 40%) above the phase transition temperature. The chemical design of LC materials has been described by White & Broer (35).

An increase in environmental temperature can induce shape deformation in LCEs. However, pristine LCEs have a relatively low thermal conductivity. Spatially controlling the thermal conduction, dissipation, and thermal gradients efficiently is necessary for long-distance power transfer. One strategy to improve the thermal response and morphological stability is to embed fillers with high thermal conductivity, such as carbon black nanoparticles in LCEs (36). In addition, fluidic channels locally incorporated on the LCE surface provide enhanced and controllable heating and

Table 1 Stimuli-responsive polymers and their stimulated signals

Polymer type	Electric field	Heat	Light	Chemical (solvent, pH)	Magnetic field
Liquid crystal polymers, polymer networks, and elastomers	•	•	•	•	
Hydrogels	•	•	•	•	•
Shape memory polymers	•	•	•		
Magnetic elastomers					•
Dielectric elastomers	•				
Ionic polymer–metal composites	•				
Ionic conducting polymers	•				
Thermal expansion actuators	•	•	•		

cooling kinetics. Pumping fluidics with different temperatures enables an LCE device to rapidly lift a weight and then relax (33) (**Figure 2*d***).

2.1.2. Photoresponsive liquid crystal elastomers. Light, as a remote, directionally controllable, and clean energy source, has been used to trigger light actuation in LC materials. The light's properties, including its wavelength, intensity, and polarization, can be customized for specific demands through spatial and temporal control. The deformation of LC materials can be triggered by either a photochemical reaction or photothermal heating. The photochemical reaction is obtained by incorporating photochromic molecules, such as azobenzene (34), spiropyran (37), or a fulgide derivative (38). For example, the azobenzene molecule has a *trans* form with a rod-like shape in the dark state and a *cis* form with a bent shape under UV irradiation. For LC materials with incorporated azobenzene guest molecules, the *trans–cis* photoisomerization of azobenzene under UV light decreases the average molecule length and destabilizes the alignment of entire LC phases, leading to an anisotropic–isotropic phase change. In other words, the effect of a configuration change in small molecules can be largely amplified to produce macroscopic deformation, with minimal energy needed to induce the photochemical reaction isothermally (**Figure 2*c***). However, an LC material that is actuated photochemically is unable to autonomously relax when the UV light stimulus is turned off. The recovery process usually requires illumination with visible light of another wavelength (**Figure 2*c***); one solution to address this issue is to specifically select a wavelength that overlaps the absorption range of *cis–trans* and *trans–cis* configurations (39).

The photothermal effect provides an alternative and efficient means of photoactuation, by converting photonic energy to heat. The photothermal effect can occur with high spatiotemporal resolution and negligible energy loss. Photothermal agents (light absorbers) can be added inside or on the surface of an LCE. The elevation of temperature induces the phase transition of the LCE from the anisotropic state to the isotropic state. The light absorbers can be carbon nanomaterials (40, 41), polydopamine (42), or metal nanoparticles (43).

Numerous light-induced LCE soft robots have been developed, such as grippers, walkers, swimmers, and self-sustained oscillators. Because photoactuation removes the need for a control circuit and power supply in the body, a photoresponsive LCE enables researchers to design untethered, battery-free, small-scaled soft robots. In this case, a relatively low light intensity (a few tens of suns) is sufficient to penetrate throughout the film, and a large actuation strain can be achieved. Compared with other materials, the molecular alignment of LCEs allows for precise control of actuation modes, leading to more versatile robotic motion and task execution. We discuss the performance of specific robots that use LCEs in Section 3.

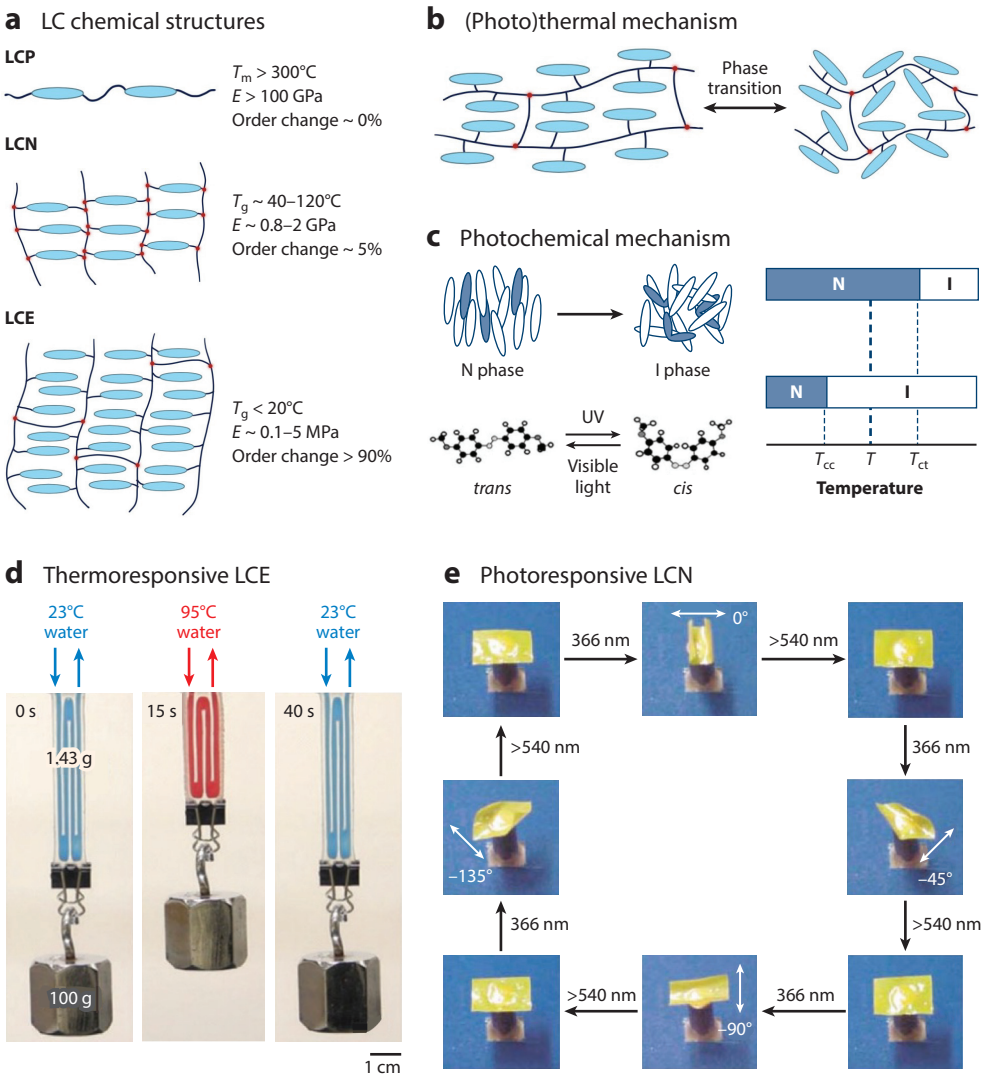

Figure 2

(*a*) Chemical structures of LC materials. T_m is the melting temperature, T_g is the glass transition temperature, and E is the modulus. (*b*) Actuation mechanisms of thermoresponsive reconfiguration in LC materials. (*c*) Photochemical reaction in LC materials. T_{cc} and T_{ct} are the phase transition temperatures of the LCN when the azobenzene molecules are in a *cis* and *trans* state, respectively. Panel adapted from Reference 32 with permission from Wiley. (*d*) Thermoresponsive LCE triggered by hot and cold fluids for object lifting. Panel adapted from Reference 33 with permission from Wiley. (*e*) Photoresponsive LCN controlled by light polarization. Panel adapted from Reference 34 with permission from Nature Publishing Group. Abbreviations: I, isotropic; LC, liquid crystal; LCE, liquid crystal elastomer; LCN, liquid crystal polymer network; LCP, liquid crystal polymer; N, nematic.

2.1.3. Electrothermal liquid crystal elastomers. Chiral smectic-A LCs exhibit the electroclinic effect, where the orientations of molecules tilt under an electric field. The LCE film can rapidly and reversibly twist out of the plane under a 16-V electric field. However, this behavior is limited to this specific molecule and has a small deformation strain (44). Another, more universal method is to induce an electrical-to-thermal energy transition (the electrothermal effect, or Joule

heating) to directly heat the material above the transition temperature. The Joule heat (Q) is affected by the applied voltage (U) and the material resistance (R), according to the formula $Q = U^2/R$. To improve the heat generation, the resistance of the material should be low.

Typically, conductive heating layers can be laminated on materials. Such a strategy benefits from facile fabrication, precise control, and low cost. The heating layers to induce the Joule heating can be a metal-mesh heater (36) or silver nanowires (45). With the patterning of an electrothermal layer, the LCE soft robot can be stimulated locally and perform complicated predefined locomotion. However, the bulk deformation relies on the thermal energy diffusing into the polymer, which will greatly decrease with increasing polymer thickness. The delamination of the multiple layers may impede the efficient actuation and stability of the robot. A more uniform heating strategy involves uniformly dispersing the conductive components inside the LCE. This strategy requires fillers so as to not restrict the LCE deformation while maintaining a low bulk resistance.

2.2. Hydrogels

Hydrogels are three-dimensional hydrophilic polymeric networks containing a high water content. In soft robotics and biomimetic applications, hydrogels have received considerable attention for two reasons: (*a*) They can swell and deswell when stimulated by water diffusion in or out of the hydrogel mesh, respectively, which can produce large volumetric changes without a tethered external power source, and (*b*) they exhibit comparable moduli (kPa) to biological tissues and organs.

A variety of stimuli-responsive hydrogels have been reviewed in the past few years (46–48). This review focuses primarily on the recent progress in hydrogels for soft robotics in terms of the materials' designs, properties, and performance. Stimuli-responsive hydrogels can respond to temperature, light, electric and magnetic fields, chemical stimuli, pH, redox reactions, and biomolecules. In this section, we focus on heat and light, which have had more robot-related investigations in academia than other mechanisms. We do not discuss electrical responsiveness here, and instead cover that aspect in Section 2.5; we also do not discuss pH-, redox-reaction-, or biomolecule-responsive gels here, considering their relatively slow responses, limited mechanical properties, and small number of demonstrations in robotic applications.

2.2.1. Thermally responsive hydrogels. Thermally responsive hydrogels are dependent largely on hydrophilicity and hydrophobicity changes at different temperatures. Some hydrogels containing both hydrophilic (e.g., amide and carboxyl) and hydrophobic (e.g., methyl ethyl and propyl) groups possess a lower critical solution temperature (LCST) (49). When the temperature is below the LCST, the hydrogel is hydrophilic and absorbs water; conversely, when the temperature is above the LCST, the hydrogel is hydrophobic and expels water due to its increased entropy, resulting in volume shrinkage. By contrast, some hydrogels, such as poly(acrylic acid–co-acrylamide), have an upper critical solution temperature (UCST). This type of hydrogel induces enthalpy-driven swelling above the UCST and shrinking below the UCST.

Poly(*N*-isopropylacrylamide) (PNIPAAm) with LCST behavior is one of the most widely developed thermally responsive hydrogels for soft actuators (**Figure 3*a***). However, the volume changes of pristine PNIPAAm hydrogel upon heating and cooling proceed very slowly, usually taking in the range of minutes to hours. This is because the polymeric mesh creates hydrophobic and impenetrable surface structures, which impedes water diffusion through the network (54). To improve the response rate, researchers have tuned the morphology of hydrogels using various techniques, including adding pore-forming templates (55), using cryopolymerization to produce large pores (56), using ice templating to introduce aligned microstructure, synthesizing a nanostructured hydrogel (50), and changing the polymerization solvents (57). However, increasing the

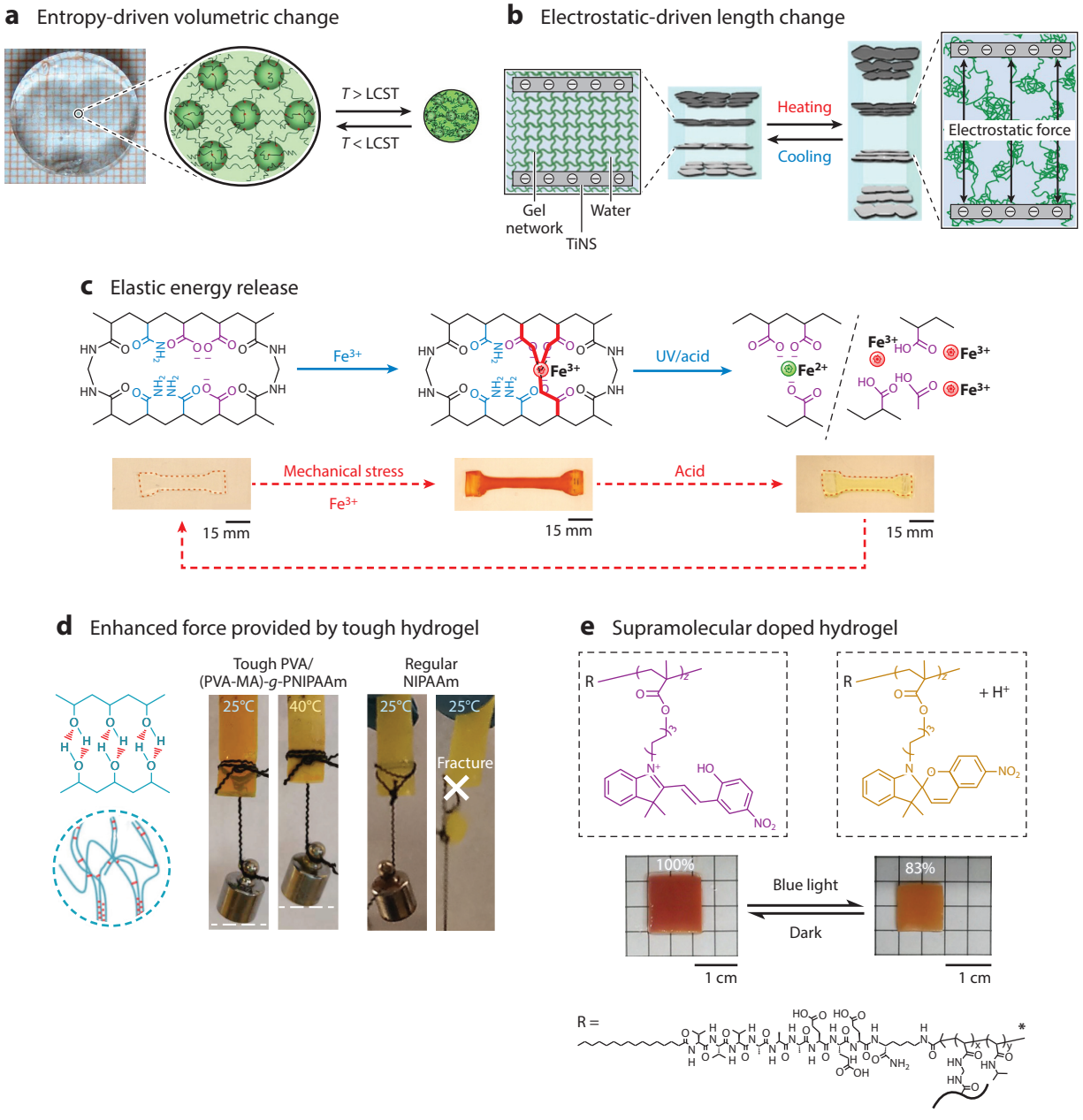

Figure 3

(*a*) Thermoresponsive hydrogel above and below the LCST. Panel adapted from Reference 50 with permission from Nature Publishing Group. (*b*) Fast actuation of hydrogel in response to heat due to the electrostatic force. Panel adapted from Reference 51 with permission from Nature Publishing Group. (*c*) Large delivered force of contractile hydrogel due to the release of prestored elastic energy. (*d*) Enhanced deliverable force through the incorporation of tough hydrogel. Panel adapted from Reference 52 with permission from ACS Publishing. (*e*) Supramolecular doped hydrogel in response to light. Panel adapted from Reference 53 with permission from Nature Publishing Group. Abbreviations: LCST, lower critical solution temperature; NIPAAm, *N*-isopropylacrylamide; PVA, poly(vinyl alcohol); (PVA-MA)-*g*-PNIPAAm, [poly(vinyl alcohol)–methacrylate]-graft-poly(*N*-isopropylacrylamide); TiNS, titania nanosheet.

pore size sacrifices mechanical strength due to the increased disconnection between networks, which is a large hurdle for soft robotics applications. Recently, the Aida group (51) has utilized electrostatic repulsion by incorporating cofacially oriented titania nanosheets in a PNIPAAm hydrogel. Upon heating, the dehydration of PNIPAAm induces a permittivity change in the system, which rapidly changes the nanosheet distance (response time of ∼1 s) and leads to anisotropic expansion of the hydrogel (**Figure 3*b***).

To improve mechanical strength, one traditional approach is to add nanofillers (58). Another approach involves incorporating a second tough polymer network formed by aggregated polymer chains (52, 59, 60) (**Figure 3*d***) and adding nanofillers. Interestingly, a second, more hydrophilic polymer network and nanoparticle fillers can facilitate water diffusion by creating water channels during swelling and deswelling, enhancing the response rate (58, 61).

2.2.2. Photoresponsive hydrogels. Extensive research has focused on developing photoresponsive hydrogels. Like in LCEs, one approach is to use photoisomerization by incorporating photoswitchable azobenzene or spiropyran molecules into the hydrogel system. Changes in supramolecular interactions at different temperatures result in changes in hydrogel volume. In addition, some photoswitchable metallopolymers embedded in the hydrogel system can trigger a photoresponsive change, where the coordinated ligand in the metal complex is replaced with another ligand under light (62). However, the actuation rates of these systems are still limited to tens of minutes to a few hours (63, 64). Li et al. (53) have reported a spiropyran and PNIPAAm hybrid hydrogel containing peptide amphiphile supramolecular polymers. Specifically, these polymers form a reversibly deformable and water-diffusing skeleton to mechanically reinforce the hydrogel network and also produce faster mass transport and an enhanced response rate (**Figure 3*f***). To further improve the light responsiveness, photothermal actuation has been widely utilized due to the heat localization, high energy conversion efficiency, fast response, programmability, and complex shape morphing. Embedding light absorbers such as graphene oxide, carbon nanotubes (CNTs), and gold nanoparticles renders the thermoresponsive hydrogel photoresponsive (57, 65, 66).

2.2.3. Response performance of hydrogels. Several hydrogel-based soft robots have been reported, such as underwater grippers (67), walkers (53), and swimmers (6). However, due to their high water content and low polymer fraction, the intrinsically limited mechanical properties and low deliverable force ($\sim 10^{-2}$ N or lower) hinder practical applications (68, 69). The diffusion-based actuation mechanism generally exhibits slow response rates and a resulting limited output power. In addition, the kinetics suffer considerably from scaling up to larger devices (a few hours at a centimeter scale). In nature, biological hydrogels such as muscle and tendon can rapidly respond to external stimuli for mechanical actuation along with providing high mechanical robustness (70). Muscle can typically generate approximately 20% strain and 100 kPa of strength, with a working density of 8 kJ/m^3. From the perspective of pursuing highly robust and reliable soft robots that have precise responses to stimuli, future investigation should focus on enhancing mechanical properties without compromising the response rate. To address this diffusion–mechanical property trade-off, our group has shown that polymerizing stimuli-responsive hydrogels in a specific co-nonsolvent system can result in hierarchically structured pores with highly interconnected pores and structurally reinforced pore walls, demonstrating simultaneously enhanced diffusive and mechanical properties (71, 72). Another approach is to pump fluids in an enclosed hydrogel-based chamber, working as a hydraulic actuation mechanism (73). Alternatively, one can rely on solvent exchange to produce volume shrinkage due to the different swelling ratios of the polymeric network in different solvents. The actuation can rapidly occur even when the hydrogel modulus is high (0.8 MPa) (74). Recently, our group reported a fast and strongly contractile hydrogel

actuated by UV light (68). To mimic the jumping of animals, we temporarily stored potential energy by prestretching and fixing the hydrogel using dynamic bonds, then rapidly released the energy upon UV stimulation to achieve a large force (40 kPa), high response rate (25% strain/min), and high working density (15.3 kJ/m^3), which even outperformed biological muscles (**Figure 3*c***).

The evaporation of water in an open-air environment may cause performance variation, and most hydrogel actuators must be operated in water. This issue can be addressed by coating the hydrogel surface with a hydrophobic shell (75). However, the actuation induced by water expulsion out of the coating might be impeded for in-air applications. The open question in this field is the specific application of the hydrogel robot. Hydrogels have properties that are comparable to those of biological systems, such as similar mechanical moduli, high water content, flexibility, and multifunctional actuation. The specific mechanical and actuation performance may be suitable for underwater applications and human–machine interfaces that benefit from the low modulus and high compliance.

2.3. Shape Memory Polymers

SMPs are a class of materials with intrinsic thermal responsiveness. After being programmed (i.e., stretched) at an elevated temperature (T_{reset}) and cooled to a low temperature (T_{low}) with a programmed shape, SMPs can store their temporary shapes by freezing the oriented crystallites of several domains. When heated to a higher temperature ($T_{high} > T_{reset}$), the temporary shape is erased and the original permanent shape is recovered. Conventionally, the temporary shape cannot be shifted back after cooling unless additional programming is conducted to create another oriented domain. Such polymers with irreversible actuation are called one-way SMPs.

In recent years, reversible SMPs with repeated shape transformations have been developed, showing greater potential for soft actuation and soft robotics. One example of inducing a reversible shape memory effect is via semicrystalline polymers, which have a wide range of melting temperatures. Microscopically, semicrystalline polymers are composed of short, soft crystalline sequences with a low melting temperature as well as long, hard crystalline sequences with a high melting temperature (76, 77) (**Figure 4*a***). To trigger the actuation, the polymer can be programmed at a reset temperature (T_{reset}) and maintain the temporary shape when cooled down. When the polymer is heated to an intermediate temperature ($T_{high} < T_{reset}$), the oriented soft crystallites melt, working as the actuation domain, while hard crystallites remain in the polymer, working as the skeleton domain. The polymer contracts as a result of the loss of partial orientation. Then the cooling causes the reorientation of soft crystallites via the entropy-driven recoiling of oriented soft domains, which allows for reversible actuation in reversible SMPs (78, 81). The reversible shape memory effect can also be produced by coupling two polymer units that have different transition temperatures, whereby the domain with the high melting temperature acts as the skeleton domain while the domain with the low melting temperature acts as the actuation domain (82). However, since the crystalline domains in the polymer are not all used for actuation, the actuation strains in reversible SMPs are relatively low.

SMPs can also be actuated through light irradiation, mainly through the photothermal mechanism. For example, Ge et al. (83) loaded poly-(ethylene-co-vinyl acetate) (EVA) with small amounts of gold nanoparticles (<0.1 wt%) and achieved reversible strip bending via the photothermal effect by illuminating it with a 532-nm green laser. The melting temperature of EVA is approximately 40°C. In another study, Wang & Zhu (84) prepared light-actuated reversible SMP composites. They incorporated very small amounts of polydopamine nanospheres (<0.15 wt%) into semicrystalline polymer networks based on biodegradable poly(ε-caprolactone) copolymers. SMPs can also be actuated via electrothermal mechanisms, such as by spray evaporation of CNTs on an SMP film (85) or vapor phase deposition of polypyrrole on an SMP film (86).

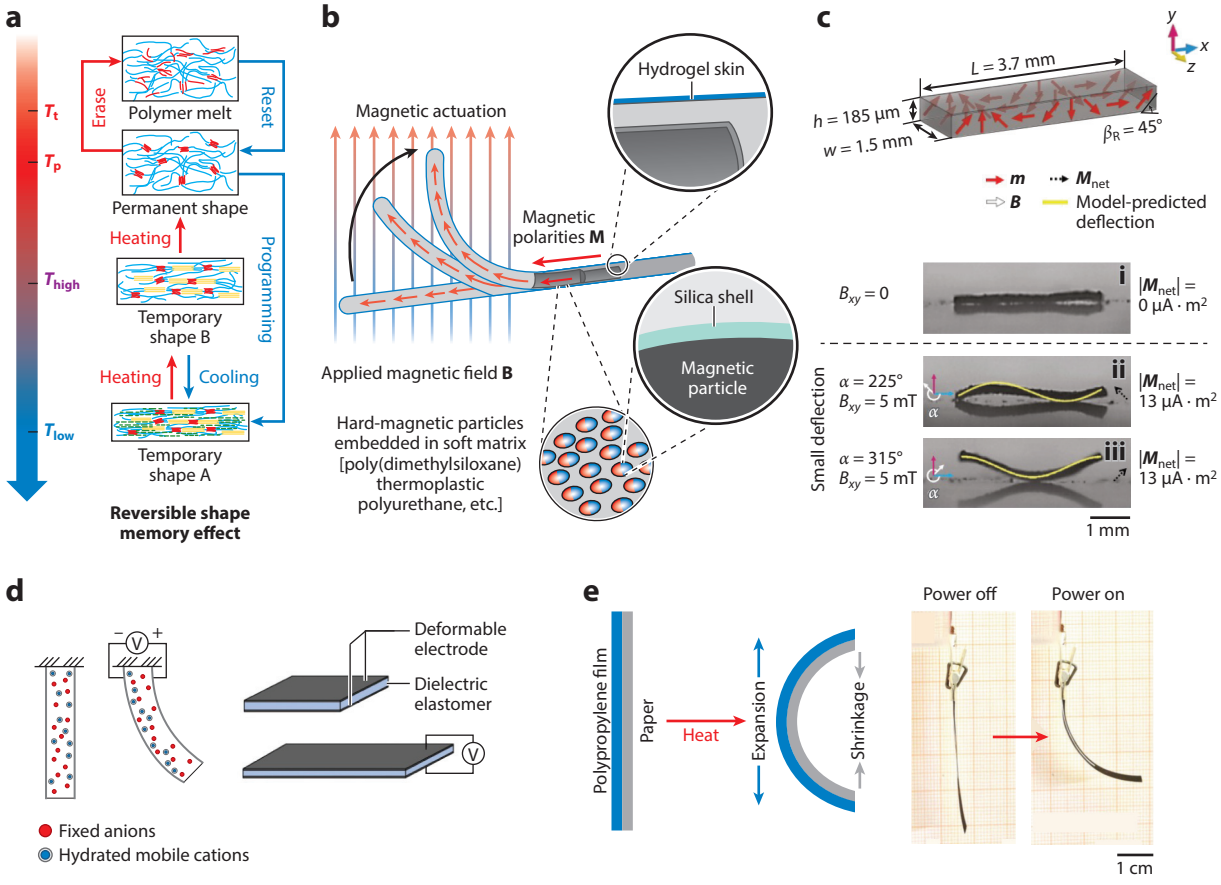

Figure 4

(*a*) Design and mechanism of reversible shape memory polymers. T_t is the temperature at which the polymer is totally melted, and T_p is the programming temperature. Panel adapted from Reference 78 with permission from ACS Publishing. (*b*) Bending motion of magnetic elastomers. Panel adapted from Reference 2 with permission from Science Publishing Group. (*c*) Traveling-wave formation of magnetic elastomers through the design of the magnetization alignment of the material. Here, **m** is the magnetization profile, **B** is the magnetic field, and $\mathbf{M_{net}}$ is the effective magnetic moment. Panel adapted from Reference 79 with permission from Nature Publishing Group. (*d*) Design and mechanism of electroactive polymers. Panel adapted from Reference 9 with permission from Wiley. (*e*) Bending mechanism and performance of thermal expansion actuators, which can be triggered by heat or by photothermal or electrothermal effects. Panel adapted from Reference 80 with permission from Wiley.

2.4. Magnetic Elastomers

Magnetic fields can penetrate through most biological and synthetic materials, enabling the operation of soft robots noninvasively and remotely in enclosed and confined spaces. In one approach, the magnetic actuators are made by simply attaching magnets to the material (87). In most cases, magnetic particles are embedded in a soft polymeric matrix such as poly(dimethylsiloxane), Ecoflex, polyurethane, or hydrogel. When a magnetic field is applied to these soft actuators, the embedded magnetic particles align with it. A magnetic elastomer matrix that has low mechanical hysteresis enables the responsive composite to readily recover its initial shape in the absence of stimuli. The deformation manipulation of magnetic actuators usually includes the spatiotemporal control of magnetic fields externally and the spatial distribution of the magnetization profile of

the robot. Since the direction and magnitude of such parameters vary, the deformation mode of the soft robot can be customized independently, including length contraction and elongation as well as angular deflection. The response to magnetic actuation can be very fast (up to 100 Hz). Due to such advantages, magnetic actuators have been demonstrated in many potential practical applications.

Recently, Hu et al. (79) demonstrated an untethered small-scale magnetoelastic soft robot composed of Ecoflex and neodymium-iron-boron particles (**Figure 4*c***). Under the manipulation of a time-dependent magnetic field, this rectangular soft robot with single-wavelength harmonic magnetization performs multimodal locomotion, such as swimming inside or on top of a liquid, jumping over obstacles, rolling over a rigid substrate, crawling, and accessing confined tunnels. The authors demonstrated complex robotic behaviors, including liquid-to-solid terrain transition and object gripping, transportation, and release. Such demonstrations verify the robustness of magnetic operation. Another interesting work involved embedding neodymium-iron-boron particles within a soft polymer matrix and fabricating the device into a fiber geometry (2). This submillimeter-diameter soft-continuum robot could be steered omnidirectionally and navigated by an external magnetic field and was capable of programmed guidance through constrained and tortuous vessels in cerebrovascular systems and the delivery of a laser fiber to a desired place. In addition, magnetic elastomers can be used as a wearable magnetic skin for eye tracking and remote gesture control via integration with other sensors (88) (**Figure 4*b***).

Another mechanism related to magnetic field operation is based on the magnetothermal effect. Applying an alternating magnetic field to magnetic particles can generate heat, and if the magnetic particles are embedded in a thermoresponsive polymer, the heat released can trigger deformation. For example, embedding Fe_3O_4 microparticles in PNIPAAm hydrogels enables the material to shrink and be used as a soft gripper under an electromagnetic field (89).

Although comprehensive robotic demonstrations have been reported using magnetic stimulation, the limitation of magnetic robots is that they require bulky external magnetic field generators, which impedes applications in large, open areas such as outdoor exploration and monitoring. In the future, magnetically responsive polymers for soft robotics could greatly benefit from onboard generation of magnetic fields instead of relying on external equipment, which would enable wireless control and let these robots be used in open spaces. One possible approach is to incorporate a coiled wire or liquid metal to provide a current to create electromagnetic induction and embed magnetic particles in the material. In addition, for scenarios where the operator cannot directly see the robot or its surroundings, the robot may rely on other observation techniques to assist in navigation, such as fluoroscopic imaging or ultrasound imaging.

2.5. Electroactive Polymers

EAPs can convert electrical energy to mechanical deformation. They have received significant attention in soft robotics due to their convenient electrical power operation, controllability, high force generation, and high power generation. Depending on the working mechanism, EAPs can be driven using ion transduction or a nonionic mechanism. For nonionic EAPs, we focus mainly on dielectric elastomers (DEs), which actuate via electrostatic force. Ionic-based EAPs include ionic polymer–metal composites (IPMCs) and ionic conducting polymers (ICPs), which rely on the diffusion of mobile ions in wet conditions. In general, nonionic EAPs can exhibit greater strength, higher strain, and faster response times in a dry state but usually need the application of thousands of volts to trigger the actuation. Ionic EAPs typically require a few volts for actuation but exhibit less strength, lower strain, and slower response times and must be immersed or encapsulated in an electrolyte solution.

2.5.1. Dielectric elastomers. DEs are characterized by their high energy density, rapid actuation (<200 μs) (90), flexibility (elastic modulus of ~1 MPa), simple fabrication, and capability to self-sense their actuation. A DE is typically composed of a thin DE film sandwiched between two layers of flexible electrodes (**Figure 4*d***). In a typical actuation mode, the electrostatic force is generated across the sandwiched structured device under the application of voltage (the electric field is 50–100 V/μm), leading to a compression in the thickness direction and an isotropic expansion in the planar direction. Prestretching and fixing the dielectric membrane along one direction enables a uniaxial deformation mode. Out-of-plane bending and buckling can also be achieved by tailoring the structure of the device (91).

For a typical isotropic expansion, the generated strain (S_x) is proportional to the dielectric permittivity (ε) and the square of the applied electric field (V) and is inversely related to Young's modulus (Y) and the square of the thickness (t_m) (92):

$$S_x = \varepsilon \frac{V^2}{2t_m{}^2 Y}.$$

Although increasing the applied voltage improves the actuation strain, the intrinsic high voltage (kV range) may result in instability issues and possible safety concerns (93). To this end, significant efforts have been made to decrease the driving voltage of DEs while maintaining good actuation performance. The motivation for driving voltage below 500 V is lower mass, size miniaturization, and the ability to use commodity surface-mounted electronic components. Methods to achieve decreased driving voltage include reducing the film thickness to only a few microns (93) or softening the dielectric material by decreasing the cross-linking density or adding plasticizers (94). However, the power density of these robots will be compromised. In addition, the permittivity can be improved by embedding microparticles (95) or through chemical modification (96). Apart from a traditional solid DE, recent works have shown that (*a*) the liquid dielectric layer exhibits higher actuation, shorter actuation time, and self-healing properties from dielectric breakdown and (*b*) the liquid electrodes demonstrate more compliant deformation and more shape change (97).

Due to the high force generation, fast actuation, and controllability of electrical power, several DEs have been developed for soft robotics, including grippers (91), crawling robots (98), underwater swimmers (99), and flying robots (100). However, commercially available DEs require high-voltage operation with bulky equipment (power supply, voltage amplifier, and controller), which imposes tethered operation and restricts device miniaturization. Therefore, there is an increasing need to develop untethered DE-based robots with control units and sufficient locomotion speed. Li et al. (99) demonstrated a manta-ray-inspired untethered DE swimming robot that possessed outstanding swimming speed. The operation of the robot was achieved with an onboard battery and voltage amplifier, and its buoyancy balanced the weights of the onboard electronics and actuator. Ji et al. (92) reported an untethered crawling robot driven by a low-voltage stacked DE, which operated at 450 V. The milder actuation condition allowed the robot to support sensors, actuators, a battery, and control circuits onboard. This ultralight (1 g) crawling robot was able to self-navigate and follow a figure pattern autonomously.

2.5.2. Ionic polymer–metal composites. A typical IPMC actuator is composed of an ionically conductive polyelectrolyte membrane sandwiched between two thin, flexible electrodes. The polyelectrolyte membrane usually contains a fixed-charge polymer chain with oppositely charged free ions. When a voltage is applied across the thickness direction of the conductive membrane, the positively charged free ions tend to accumulate on the cathode side. Such a nonuniform distribution of ions causes an osmotic pressure difference, leading to a bending of the device (**Figure 4*d***). IPMCs are good candidates for soft robots because of their low operation voltage, fast response

time (0.1 s), and high deformation (40%). However, they require encapsulation to improve performance in dry air and prevent water leakage out of the electrode. Their low actuation bandwidth and high cost also need to be addressed.

2.5.3. Ionic conducting polymers. Conjugated polymers are polymers with alternating single and double bonds along the polymer chain, which endows them with unique electronic conduction. Classic conducting polymers (CPs) include polyaniline (101), polypyrrole (102), and poly(3,4-ethylenedioxythiophene) (103). CPs can be driven electrochemically via oxidation or reduction in ionic electrolyte. During the redox reaction under an electric field, CPs undergo doping or dedoping, whereby electrons are added or removed along the polymer chains. To maintain charge neutrality, the process results in the movement of cations and anions in the CP's network, which contributes to macroscopic mechanical deformation (104). In an anion-transporting p-type CP, oxidization induces the attachment of anions and the expansion of the CP, while reduction allows the CP to shrink. ICPs feature low operation voltage, flexibility, negligible self-discharging, and easy fabrication. In the electrochemical model, the conductive nature of CPs also endows them with self-sensing actuation behavior, demonstrating the potential for proprioception (105). However, they suffer from relatively poor cyclic stability and oxygen sensitivity and can only operate in an aqueous environment.

2.6. Thermal Expansion Actuators

Materials naturally expand or shrink in response to temperature changes, characterized by the coefficient of thermal expansion (CTE). Carbon materials such as CNTs, reduced graphene oxide, and graphite have a relatively low CTE compared with polymers, such as poly(vinylidene fluoride), poly(dimethylsiloxane), and polycarbonate (106). Integrating CNTs and poly(dimethylsiloxane) into an asymmetric bilayer structure as an exemplary system enables the film to bend toward the CNT side by direct heating or via the photothermal effect. By depositing silver nanowires on a low-density polyethylene and poly(vinyl chloride) bilayer, Kim et al. (107) demonstrated soft grippers induced by Joule heating, enabled by the large CTE difference of the two layers. A combination of graphite microparticles and CNT ink deposited on paper was also capable of deforming upon Joule heating. Interestingly, the received electrical signal from the voltage application can be used to sense the device's own deformation, demonstrating self-sensing actuation behavior (80) (**Figure 4*e***). These types of actuators illustrate the advantages of easy fabrication, diverse stimulus compatibility, and multifunctional deformation. However, the actuators are typically thin, usually exhibit low generated force, and may experience delamination during operation.

3. ROBOTIC APPLICATIONS

3.1. Grasping

Human fingers can grasp objects quickly and accurately and have the flexibility and dexterity to conform to different objects' shapes without breaking them. An increasing number of studies on shape-morphing actuators have reported soft robots that were able to pick up and hold objects via on–off switching of the stimuli. On the one hand, the mechanical properties of the materials, such as their stiffness, deformation, deliverable force, and grasping speed, need to be investigated. On the other hand, the device design and engineering of soft grippers are also essential for meeting the requirements for grasping, including their texture, surface stiffness, lightness, tethered or untethered design, size miniaturization, biocompatibility, operating environment (e.g., in air or in water), and system complexity (integration of sensors and controllers).

Among the choices of materials for soft grippers, stimuli-responsive polymers can transform their shapes into curved, folded, or rolled structures in response to external signals without manual control. Stimuli-responsive polymers for soft grippers have been broadly discussed in a previous review (109). This section concentrates primarily on the working mechanisms, device architectures, and gripping performance.

3.1.1. Gripping by stimuli-responsive actuation. The majority of gripping actuation is based on the out-of-plane folding of smart materials. Under stimuli, the actuator exhibits asymmetric deformation that converts the two-dimensional thin, flat shape to a three-dimensional curved, self-folded, or rolled shape. The most extensively utilized design is the bimorph structured film, which contains an active layer with stimuli responsiveness and a passive layer to provide the strain difference. The bending ratio is determined by the layer dimensions, mechanical properties, and actuation properties of the layers. Due to the simplicity of the design, multiple stimuli can trigger the gripping motion. When graphene oxide, single-wall CNTs, or other nanoparticles are embedded in hydrogels, hydrogel soft grippers can respond to pH, light, ionic strength, and temperature change (65) (**Figure 5*a***). The soft grippers can be operated via the electrothermal mechanism. Kim et al. (107) demonstrated multilayer materials composed of silver nanowires, low-density polyethylene, and poly(vinyl chloride). The electrical-to-heat transduction from the silver nanowire layer can produce a CTE difference for bending (2.5/cm at 40°C).

Alternatively, folding can be achieved by manipulating a single material with an anisotropic microstructure. The cross-linking density gradient along the thickness direction can trigger anisotropic bending, whereby the film bends toward the side with high cross-linking density, as shown in the poly(acrylic acid)/PNIPAAm actuator (65). In addition to the polymerization gradient, Gladman et al. (110) demonstrated a four-dimensional printed anisotropic hydrogel with a programmable morphology, which was achieved by aligning reinforced cellulose fibrils through nozzle extrusion (**Figure 5*d***). Due to the heterogeneous stiffness and swelling ratio from the structural anisotropy, the researchers designed bilayers using a single material with two different directional orientations to realize bending or rolling deformation. Using a similar working principle, Fang et al. (113) utilized electrospinning to fabricate an anisotropic PNIPAAm hydrogel and laminated the layers with different orientations. In addition, a single-layer LC material with a microscopic configuration difference along the thickness direction can trigger bending, as achieved in a splay-aligned film (114). During actuation, different thermal expansions are created at the two surfaces of the film with an orientation difference, resulting in spontaneous bending of the film. Wani et al. (115) utilized a laser projector with a polarizer to program the alignment of an LCP film, performing customizable photoresponsive bending. More interestingly, a biomimetic artificial flytrap based on this material has been further demonstrated: A light beam emitted from the gripper center is scattered or reflected by the object surface back to the actuator surface, resulting in the bending of the actuator (109) (**Figure 5*b***). Therefore, such a photoresponsive gripper can autonomously recognize an object and grasp it by creating an optical feedback loop. This demonstration may trigger the design of biomimetic soft robots with autonomy and intelligence.

Furthermore, bending can be achieved by applying a directional stimulus to an isotropic smart material. Our group has recently demonstrated a sunflower-inspired soft robot that can autonomously bend and track the direction of incoming light (57) (**Figure 5*c***). The bending actuation is based on the localization of the photothermal effect on a uniform and symmetric hydrogel pillar, in which the light cannot fully penetrate the pillar. A temperature gradient is produced that results in a volumetric shrinking gradient across the thickness direction. Light tracking is achieved via a built-in feedback control, whereby overbending will self-shadow part of the light, allowing for recovery, and underbending will expose more light, allowing for greater

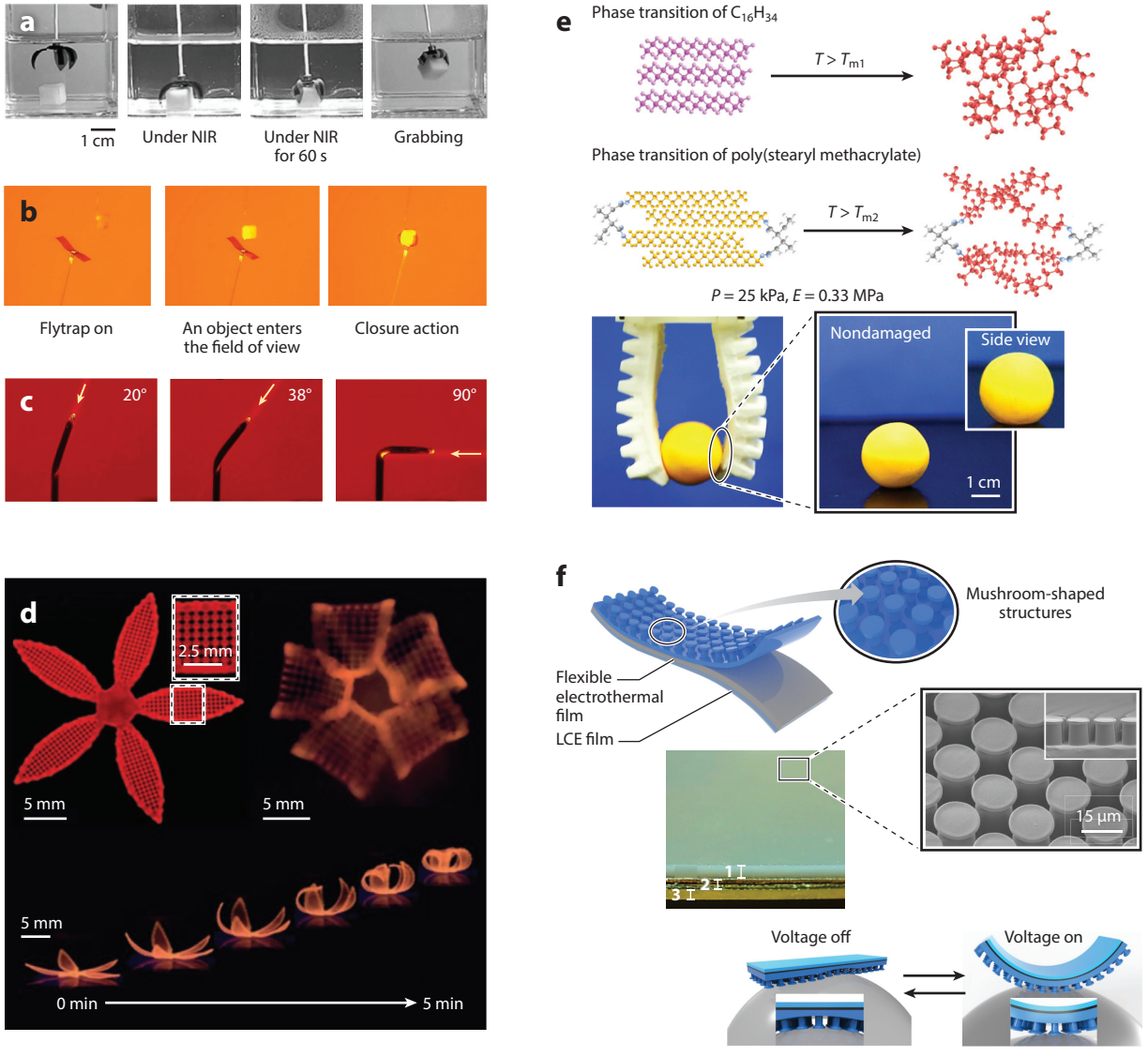

Figure 5

(*a*) Underwater grasping by hydrogel actuators triggered by the photothermal effect. Panel adapted from Reference 65 with permission from Wiley. (*b*) Autonomous grasping by an LCN-based robot using light self-shadowing. Panel adapted from Reference 109 with permission from Nature Publishing Group. (*c*) Phototracking of hydrogel toward an incident light source. Panel adapted from Reference 57 with permission from Nature Publishing Group. (*d*) Biomimetic flower blooming of a hydrogel actuator. Panel adapted from Reference 110 with permission from Nature Publishing Group. (*e*) Dynamic stiffness change of a soft grasper in response to temperature. T_m is the chemical's melting temperature, P is the pressure, and E is the modulus. Panel adapted from Reference 111 with permission from Science Publishing Group. (*f*) Use of a gecko's foot effect to enhance the adhesion of an LCE soft grasper. Panel adapted from Reference 112 with permission from the Royal Society of Chemistry. Abbreviations: LCE, liquid crystal elastomer; NIR, near infrared.

bending. The phototracking mechanism can be used for gripping, but the incident light direction must be controlled to allow for the desired folding direction.

3.1.2. Gripping by stiffness change. In nature, sea cucumbers can dynamically and reversibly tune their strength inside the multiphase dermis. Inspired by this phenomenon, controllable stiffness in soft grippers has been demonstrated that is capable of changing the material's rigidity in response to stimuli. Specifically, the actuator first envelops itself around an object in a softened state; subsequently, the on-demand stiffness change of the actuator reinforces the mechanics of the gripper, enabling the robot to hold and pick up the object. For example, an SMP with spatially patterned liquid metal wires can help control the gripping force and recognize the shape of an unknown object through electrothermal stiffness control (113). Zhuo et al. (111) demonstrated an organohydrogel with a multistage phase transition at different temperatures; by integrating the organohydrogel onto the surface of a pneumatic actuator, the authors were able to tune the stiffness of the organohydrogel surface to adapt to the local substrate modulus without damaging the target (**Figure 5*e***).

3.1.3. Gripping by adhesion change. Gecko feet can strongly adhere to any type of surface due to their nanostructured fibers (spatulae), which allow for high surface adhesion. A soft gripper can be designed with a controllable surface force like that of gecko feet (termed gecko adhesive). In particular, the adhesion-based soft gripper contains a layer of a nanostructured pattern. During bending or unbending in response to external stimuli, the average nanostructure spacing is changed, resulting in attachment or detachment (112) (**Figure 5*f***). This operation is advantageous for objects that contain a flat surface or cannot withstand high compressive force. However, the adhesion and gripping performance is limited when the surface is rough and wet.

3.2. Walking

Earthworms, snails, and caterpillars can deform their bodies in the form of a traveling wave to adapt to different environmental confinements. Inspired by these soft animals, many works have focused on mimicking caterpillar locomotion for crawling. Shape memory alloys and DEs have been designed as caterpillar-like robots, which exhibit fast responses and robust operation (116, 117). However, they usually require external power via wires or tubing and can be challenging to miniaturize. Many groups have reported LCE-based caterpillar robots stimulated by light, benefiting from untethered operation and facilitating the fabrication of micrometer-sized robots. By designing the LCE film to be wave-like or arch-like in shape, soft robots can directionally move under a cyclically scanned light pattern (**Figure 6*a***). The frictions between the surface and the robot's front body and back body differ, resulting in directional motion. Tuning the scanning light pattern and the laser power provides easy control over the traveling locomotion speed and maneuverability (41, 118). Another way to achieve directional locomotion is by setting the robot on a grating surface, such that a uniform and alternating light beam can be used without spatial control, as demonstrated by Zeng et al. (123); on a grating surface, this robot was able to walk 2.5 times as fast as it could on a paper surface.

The aforementioned walking robots are powered by periodically switching the stimulus on and off or cyclically scanning the material back and forth. An interesting research approach is to fabricate autonomous locomotive robots fueled by constant environmental energy stimuli. The Broer group (119) has clamped a fast-responding azobenzene-based LCN film to a passive frame and created wave-like locomotion under a constant light stimulus applied at an angle (**Figure 6*b***). The locomotion can be regarded as a special case of self-oscillation based on the principle of self-shadowing when the film overbends (discussed further in Section 3.4). The

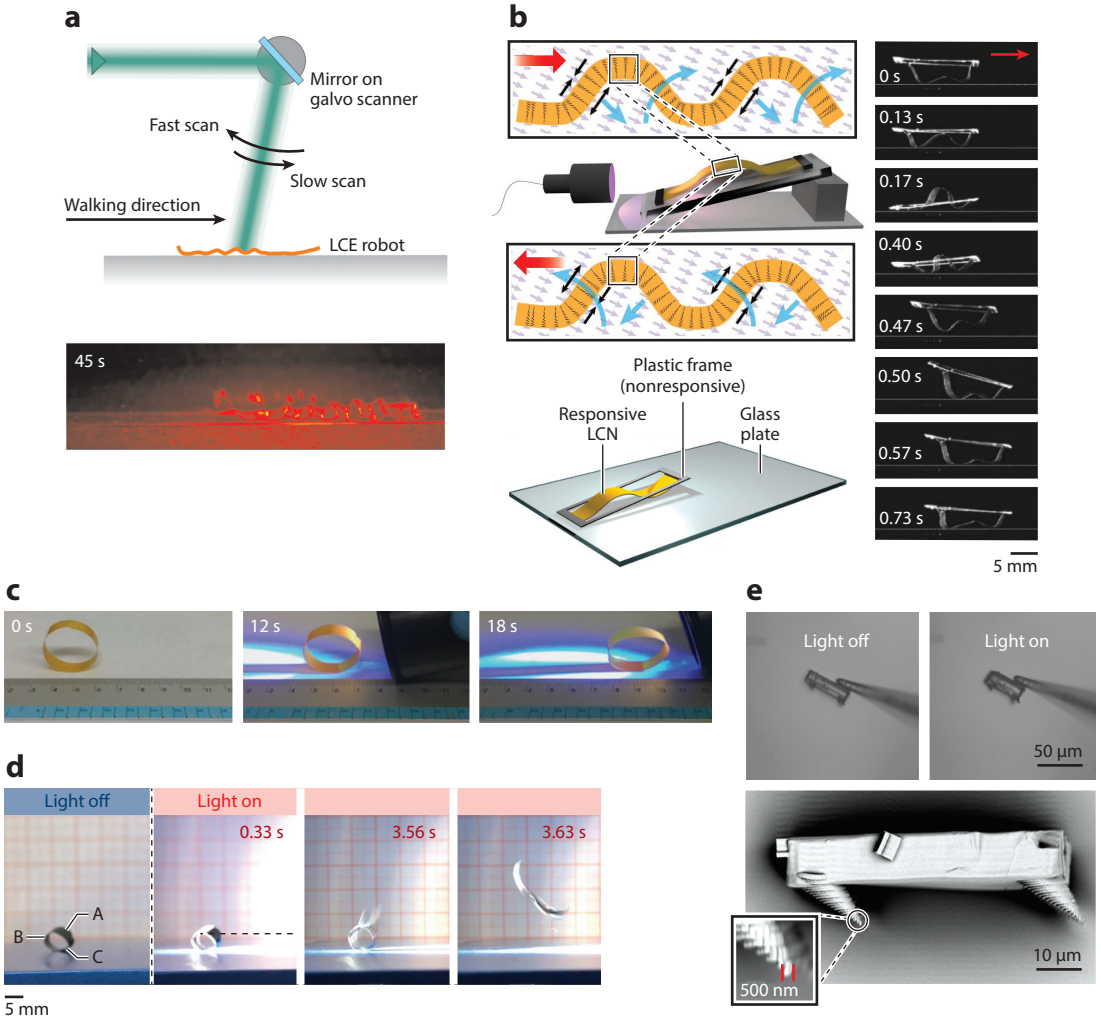

Figure 6

(*a*,*b*) Wave-propagating crawling robots based on photoresponsive LCEs, which are triggered by scanned patterned light (panel *a*) or constant light input (panel *b*). Panel *a* adapted from Reference 118 with permission from Wiley; panel *b* adapted from Reference 119 with permission from Nature Publishing Group. (*c*,*d*) Rolling (panel *c*) and jumping (panel *d*) of soft robots in response to light. Panel *c* adapted from Reference 120 with permission from Wiley; panel *d* adapted from Reference 121 with permission from Wiley. (*e*) LCE microscopic walking robot. Panel adapted from Reference 122 with permission from Wiley. Abbreviations: LCE, liquid crystal elastomer; LCN, liquid crystal polymer network.

propagation of the wave, induced by light, self-propels the device to directionally move, showing substantial potential for smart photomechanical applications.

Jumping has been demonstrated to be more efficient than crawling for terrestrial locomotion. This is usually achieved by storing elastic energy in legs stuck on a rough surface or attracted by magnets. When the elastic energy is large enough, environmental fluctuations cause the energy to be released and converted into kinetic energy, allowing the robot to jump long distances (41, 121, 122) (**Figure 6*d***). Rolling presents an alternative directional locomotive mode for terrestrial environments. During light illumination on a photoactive polymer, an asymmetric deformation

is created on the polymer surface, creating a shift in the robot's center of gravity and allowing for rolling (120, 124) (**Figure 6*c***).

It is rather challenging to realize walking at the microscopic scale, because the van der Waals and capillary forces are not negligible and create strong adhesion to the surface. For example, a $60 \times 30 \times 10\ \mu m^3$ LCE robot with four tilted legs has been fabricated to create an adhesion asymmetry for directional walking (122) (**Figure 6*e***). On a smooth, clean glass substrate, the robot can successfully walk directionally in response to a light stimulus. However, environmental fluctuations can be more dominant when the substrate is not uniform, and the walking can become random or dominated by surface conditions.

3.3. Swimming

Researchers have been inspired by nature to design swimming soft robots. At the microscale in low-Reynolds-number fluids, the motion of a microrobot is determined by nonreciprocal body motion when the contribution from viscosity is more dominant than that of inertia. In other words, nonreciprocal motion needs to be performed so that a net fluidic flow can be produced to propel the robot forward (125).

Screw-like motion, where a soft robot rotates its body in a helical fashion, like a flagellum, is considered to be the most efficient mechanism for creating nonreciprocal motion. Researchers have used gold nanoparticle–PNIPAAm hydrogels to generate helical deformation induced by photothermal heating (126, 127) (**Figure 7*a***). Magnetic robots have also been demonstrated for helical swimming under rotating, low-strength magnetic fields, showing the potential for untethered medical applications with three-dimensional control (131). The second mechanism for generating nonreciprocal motion consists of creating a traveling-wave deformation, inspired by ciliates. By periodically scanning a structured light pattern, a cylinder-shaped LCE microrobot can deform like a propagating wave to propel itself without additional forces (**Figure 7*b***). However, the speed is limited to ~0.1 body lengths/min (128). Diller et al. (129) reported a millimeter-scale magnetically responsive swimming robot using the traveling-wave mechanism, which showed significantly improved speed (**Figure 7*c***).

Another mechanism consists of a vibrating motion at a water–air interface, where a soft robot beats its flexible tail like a fish. Due to the facile operation of this mechanism, many related works have been reported in recent years. IPMCs are particularly promising actuating materials for soft swimmers because of their low operation voltage, relatively high force, and water compatibility. Using an IPMC as the vibrating tail and incorporating electronic components inside the body, including an onboard battery and mobile control unit, a soft robot can swim at high speeds (up to 20 mm/s) (132, 133). In recent years, a DE-based soft electronic fish has also been reported. By integrating a battery and high-voltage amplifier, this robot could swim untethered with a forward speed of 6.4 cm/s (0.69 body lengths/s) (99) (**Figure 7*d***). Light has also been used as an energy source to remotely power and maneuver the motion of a swimmer based on photoresponsive materials. One example consisted of an LCP actuator, with the bending tail stimulated by periodic irradiation of light on both sides of the actuator (130) (**Figure 7*e***). However, the alternating stimulation impedes its controllability and application. Recently, our research group has demonstrated a phototactic-hydrogel-based soft swimmer fueled by a constant light source. The swimmer is composed of a soft body, allowing it to float on the water–air interface, and a long, strip-like hydrogel tail. Due to the fast response of the hydrogel, the tail could perform nonequilibrium self-sustained oscillation through irradiation with a constant light source. Such autonomous oscillation could provide sufficient propulsion force for swimming away from the light source, demonstrating a speed of approximately 1.5 body lengths/min (6) (**Figure 7*f***).

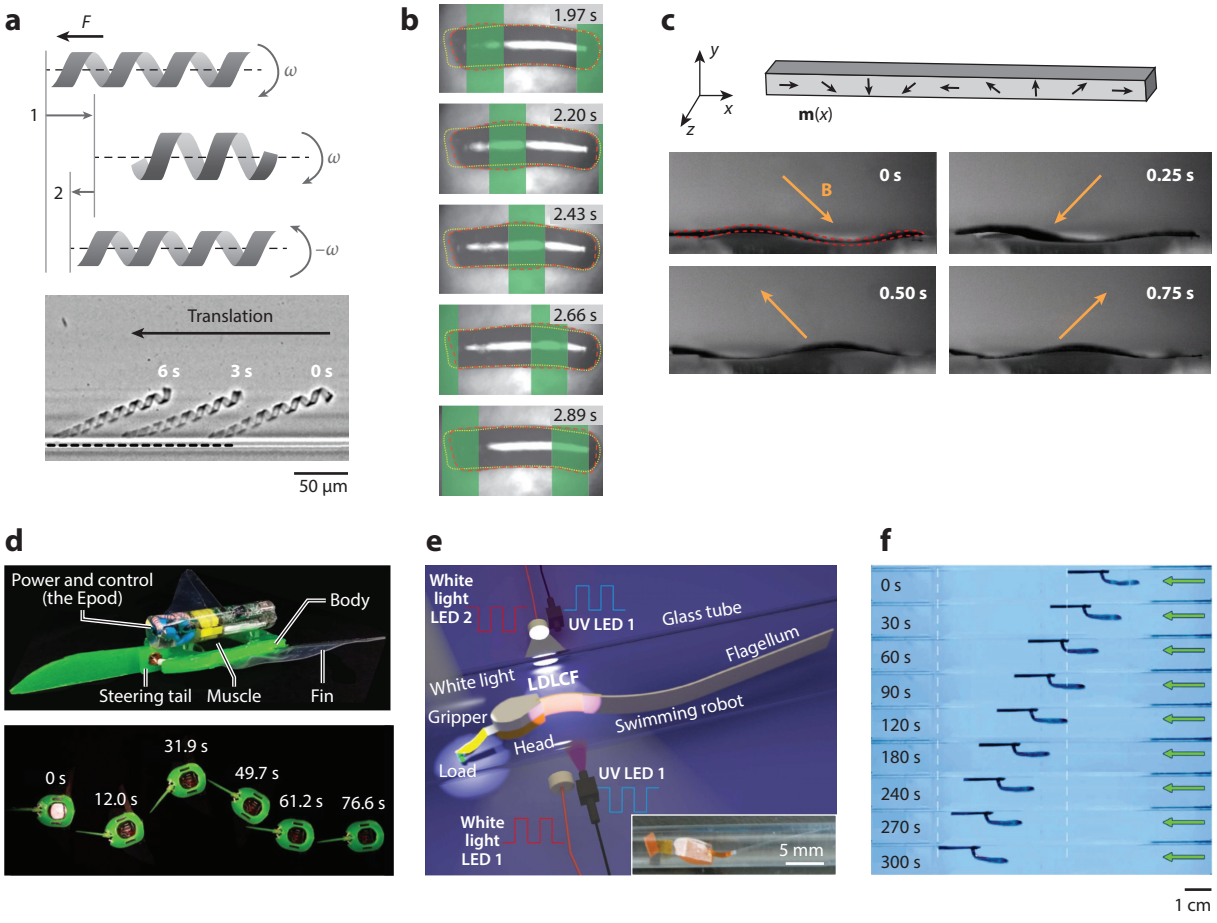

Figure 7

(*a*) Helical motion of a microscopic swimming hydrogel robot. *F* is drag, and ω is the angular frequency of rotation. Panel adapted from Reference 127 with permission from Wiley. (*b*) Traveling-wave motion of an LCE robot. Panel adapted from Reference 128 with permission from Nature Publishing Group. (*c*) Traveling-wave swimming of a magnetic elastomer robot. **B** is the magnetic field, and **m**(*x*) is the magnetization profile. Panel adapted from Reference 129 with permission from AIP Publishing. (*d*) Onboard power and control of an IPMC-based robot. Panel adapted from Reference 99 with permission from AIP Publishing. (*e*) Flapping motion of an LCE-based swimmer by pulsed light input. Panel adapted from Reference 130 with permission from Nature Publishing Group. (*f*) Self-oscillating hydrogel soft swimmer powered by a constant light source. Panel adapted from Reference 6 with permission from Science Publishing Group. Abbreviations: Epod, electronic pod; IPMC, ionic polymer–metal composite; LCE, liquid crystal elastomer; LDLCF, light-driven liquid crystal film.

To further improve swimming performance, several factors need to be considered. From the perspective of material properties, one may design stimuli-responsive materials with fast response, fast recovery, and large deformation. Regarding the mechanism of response, the thermal conductivity of water is approximately 20 times that of air, and a lot of thermal energy will be dissipated to the surrounding water bath during the robot's operation. This indicates that a higher amount of energy is required to elevate the thermally responsive materials, such as PNIPAAm hydrogel, LCEs, and SMPs, to their corresponding phase transition temperatures. Therefore, a reversible photochemical mechanism, electrical response, or magnetic response may be alternative choices for more energy-efficient and higher-performing untethered swimming robots. Furthermore, the trajectory of nonreciprocal motion is essential to produce efficient directional motion in a

low-Reynolds-number fluid; one example is to manipulate the moving mode in an artificial cilia system to maximize the generated fluidic flow (134). This may catalyze further research in the design of fast-swimming robots based on stimuli-responsive materials.

3.4. Flapping and Flying

Flying animals such as honeybees and hummingbirds can rapidly and continuously vibrate their wings, fueled by constant chemical energy. This implies that a biomimicking soft actuator must possess a high power density and high frequency to lift the body off the ground, while incorporating a sensing component for closed-loop flight control. A DE was successfully demonstrated as a power component to enable the flight of a microrobot (power density > 600 W/kg, frequency > 500 Hz) (100) (**Figure 8*a***). Compared with conventional piezoceramic actuators, this device is more tolerant of collisions due to its high compliance and resilience. With feedback control, it is able to steadily ascend and hover.

To induce such high-frequency oscillation motion in artificial responsive materials, researchers rely on manually switching the stimuli on and off. In other words, intermittent power transmission

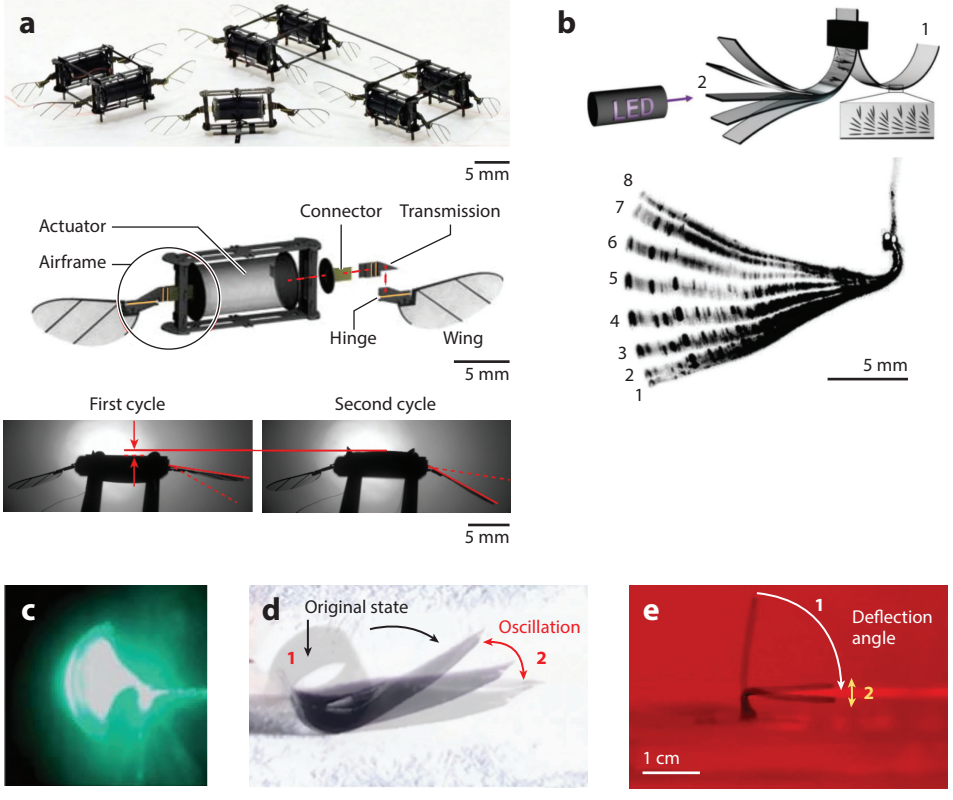

Figure 8

(*a*) Flying robot actuated by electrical power. Panel adapted from Reference 100 with permission from Nature Publishing Group. (*b–e*) Light-triggered self-sustained oscillators fabricated by a photothermal LCN (panel *b*), a photochemical LCN (panel *c*), a thermal expansion actuator (panel *d*), and a hydrogel (panel *e*). Panel *b* adapted from Reference 135 with permission from Wiley; panel *c* adapted from Reference 136 with permission from the Royal Society of Chemistry; panel *d* adapted from Reference 137 with permission from Wiley; panel *e* adapted from Reference 6 with permission from Science Publishing Group. Abbreviation: LCN, liquid crystal polymer network.

or variation in the stimuli is typically used to generate high-frequency reversible deformation. This requires the material to deform between two or more states reversibly at tens or hundreds of hertz. In the past 10 years, self-sustained mechanical oscillation powered by consistent stimuli has been widely reported, with the aim of designing soft robots with autonomous control. For example, a photoresponsive actuator exhibiting a fast response rate and recovery can produce unsteady oscillation through the self-shadowing mechanism. The material is usually constructed in a high-aspect-ratio geometry, such as a strip or cylinder, and the light is applied at an angle. Under illumination, the actuator first bends toward the light due to the deformation gradient along the thickness direction; the slight overbending of the actuator tip then blocks the illumination site, leading to a recovery of the strip; and the underbending of the strip then allows the light to expose the illumination site again, leading to bending once again. The response mechanism has been demonstrated to be highly universal, encompassing both photochemical (138) (**Figure 8*c***) and photothermal (135) (**Figure 8*b***) actuation. The material selection can be general, consisting of LC material (136), hydrogel (6) (**Figure 8*e***), or thermal expansion actuators (137) (**Figure 8*d***). Depending on the light–matter interaction, the actuation mode can be regular in-plane oscillation (138), out-of-plane torsional oscillation (139), or even chaotic motion (140). The oscillation frequency can range from 271 Hz to 0.2 Hz, around the natural frequency of the material and governed by the mechanical properties (6, 136) as follows:

$$f = \frac{3.5}{8\pi}\frac{t}{L^2}\sqrt{\frac{E}{\rho}},$$

where t is the thickness, L is the length, E is the Young's modulus, and ρ is the density of the material.

The angular amplitude can be finely controlled from a few angles to almost 90°, largely determined by light intensity and environmental resistance (136). Self-oscillators in response to other stimuli, such as humidity (29) and thermal (141) gradients, have also been reported. With this recent insight into self-oscillators, automated wings in flying robots can be anticipated.

Although promising, achieving a flying soft robot based on stimuli-responsive materials is incredibly challenging. First, one needs to design self-oscillation with a high power density and high frequency, which requires the material to be highly responsive to stimuli. The trajectory of the flapping wings must be optimized to provide maximum thrust, which can overcome air resistance and support the device's own weight. In addition, the robotic structure and mechanism need to be carefully designed to allow the stimulus to constantly power the soft robot's oscillation. We expect that a stimuli-responsive smart flying soft robot can be demonstrated in the future with the knowledge and understanding of current responsive materials coupled with structural designs from reported electrically powered aerial robots (142, 143).

3.5. Somatosensory Actuators

Biological systems demonstrate manual dexterity and motor skills to adapt to changing environments. They can perceive the environment by exteroception, via stimuli such as static pressure, dynamic vibration, pain, and temperature. The self-movement and body position can also be sensed through proprioception. These physical sensing activities rely on receptors for sensation and effectors for response, through a reflex feedback or neuromuscular mechanism. By mimicking the perception and stimuli-responsive motility in somatosensory systems, the emerging field of soft robotics has replicated the functionalities for various applications, such as proprioceptive grasping (18), locomotion (144), monitoring of surface roughness (145), and object temperature (20) (**Figure 9*a***). Both open-loop (triggered by a predetermined signal without feedback) and

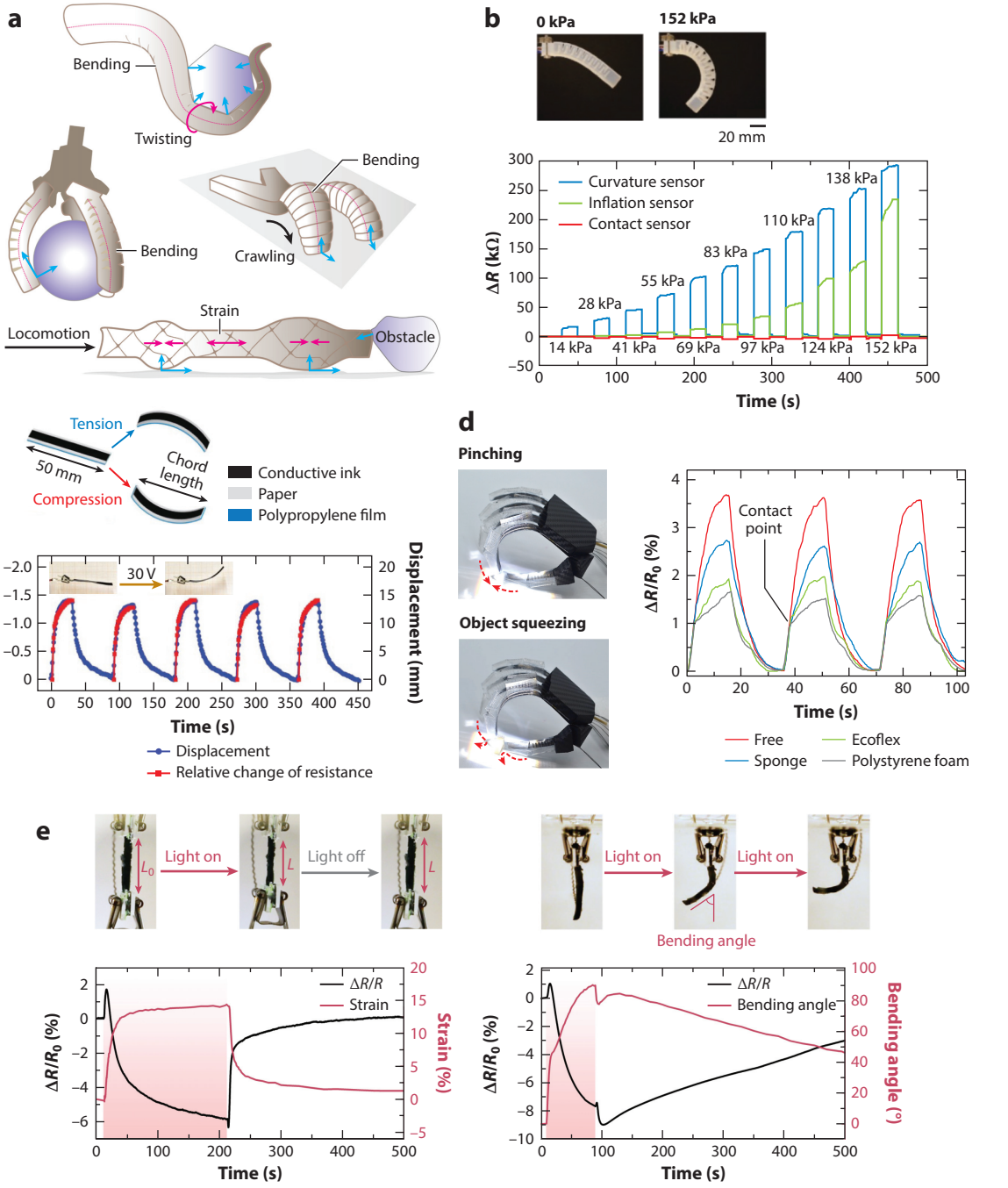

(Caption appears on following page)

Figure 9 (*Figure appears on preceding page*)

(*a*) Proprioception mode of self-sensing actuators. Panel adapted from Reference 20 with permission from Wiley. (*b*) Somatosensory pneumatic actuator. *R* is resistance. Panel adapted from Reference 18 with permission from Wiley. (*c*) Thermal expansion actuator capable of actuation and sensing deformation simultaneously. Panel adapted from Reference 80 with permission from Wiley. (*d*) Light-induced bending and perception of deformation. Panel adapted from Reference 18 with permission from Wiley. (*e*) Underwater photothermal contraction and bending with real-time sensing. Panel adapted from Reference 146 with permission from Science Publishing Group.

closed-loop (the input signal is adjusted by sensory feedback) control have been reported. The majority of reported somatosensory actuators are based on physically integrating elastomer-based pneumatic actuators with sensor components, such as a soft optical fiber (145), electroluminescent sensor (147), triboelectric sensor (144), or piezoresistive sensor (18) (**Figure 9*b***).

In recent years, bimorph structures based on CTE differences have been demonstrated as somatosensory smart actuators. They are composed of a conductive layer, for sensation, and a passive layer, for producing bending deformation via CTE mismatch. Examples of these structures include a graphene/CNT/paper actuator (80) (**Figure 9*c***), graphene oxide actuator (148), and poly(vinylidene fluoride)/polydopamine-capped reduced graphene oxide/CNT actuator (149) (**Figure 9*d***).

However, these physically integrated systems with material interfaces may experience issues with delamination and limitations of the predefined actuation mode. Therefore, it would be desirable to explore a multifunctional material by chemically integrating sensation and actuation components at the molecular level rather than at the system level. Ideally, the fully integrated system can significantly decrease the complexity, catalyzing the development of perceptive soft robots. Recently, our group has developed a chemically innervated somatosensory actuation hydrogel composed of a CP and PNIPAAm (146). The engineered microstructure gave the material an electrical conductivity that was three orders of magnitude higher than that of control samples. At higher temperatures, the volumetric shrinkage of PNIPAAm results in a conductivity change of the CP, which enables the detection of the deformation. Based on the piezoresistive mechanism, we have demonstrated open-loop and closed-loop sensing of contraction and bending underwater (**Figure 9*e***).

Besides piezoresistivity, the capacitive-based mechanism is also advantageous for constructing somatosensory devices, mainly due to their simple designs and their ability to house sensing arrays, like electronic skins. We also anticipate that optical transductors can be readily coupled with smart materials, enabling the monitoring of small deformations with high accuracy (150). Generally speaking, new innovations in somatosensory actuators are needed, such as multimodal sensor systems, multifunctional actuators, and new integration strategies.

4. CONCLUSION

In this review, we have discussed representative stimuli-responsive polymers with potential in soft robots and elaborated on their potential applications using different material systems. We aimed to provide a clear picture of the field regarding the features of each material; their current limitations; and potential directions toward reliable, robust, fast-responding, significantly deformable, and multifunctional soft robots. Regarding the development of each material and specific type of robot, we summarized and discussed the working mechanisms and the resulting performance.

Despite all these achievements, soft robotics based on stimuli-responsive polymers is still in its infancy, with many challenges left to be addressed. For example, LCEs exhibit a tunable actuation temperature and response rate but are limited by complicated fabrication and a requirement for alignment. Hydrogels exhibit multifunctionality and versatility in chemical modification but

usually suffer from diffusion-limited kinetics, low power/energy densities, and environmental restrictions. SMPs have been designed to be reversible but have a limited actuation strain. EAPs exhibit a highly compact design, high energy/power generation, easy fabrication, and accurate controllability but require a tethered design. Magnetic elastomers possess distinct controllability and versatile actuation but require a bulky supply unit. Addressing these challenges and fully utilizing the features of each material can allow scientists and researchers to pursue meaningful real-world applications, such as space exploration, environmental monitoring, structural maintenance, social assistance, security, and so on. We believe transformative impacts will be made with future breakthroughs in soft stimuli-responsive actuation, system integration, control, and soft robot autonomy.

DISCLOSURE STATEMENT

The authors are not aware of any affiliations, memberships, funding, or financial holdings that might be perceived as affecting the objectivity of this review.

ACKNOWLEDGMENTS

The research was supported by the National Science Foundation award 1724526, Office of Naval Research award N000141712117, and Air Force Office of Scientific Research grant FA9550-17-1-0311.

LITERATURE CITED

1. Brown E, Rodenberg N, Amend J, Mozeika A, Steltz E, et al. 2010. Universal robotic gripper based on the jamming of granular material. *PNAS* 107:18809–14
2. Kim Y, Parada GA, Liu S, Zhao X. 2019. Ferromagnetic soft continuum robots. *Sci. Robot.* 4:eaax7329
3. Horchler AD, Kandhari A, Daltorio KA, Moses KC, Ryan JC, et al. 2015. Peristaltic locomotion of a modular mesh-based worm robot: precision, compliance, and friction. *Soft Robot.* 2:135–45
4. Seok S, Onal CD, Cho K, Wood RJ, Rus D, Kim S. 2013. Meshworm: a peristaltic soft robot with antagonistic nickel titanium coil actuators. *IEEE/ASME Trans. Mechatron.* 18:1485–97
5. Wehner M, Truby RL, Fitzgerald DJ, Mosadegh B, Whitesides GM, et al. 2016. An integrated design and fabrication strategy for entirely soft, autonomous robots. *Nature* 536:451–55
6. Zhao Y, Xuan C, Qian X, Alsaid Y, Hua M, et al. 2019. Soft phototactic swimmer based on self-sustained hydrogel oscillator. *Sci. Robot.* 4:eaax7112
7. Jafferis NT, Helbling EF, Karpelson M, Wood RJ. 2019. Untethered flight of an insect-sized flapping-wing microscale aerial vehicle. *Nature* 570:491–95
8. Rich SI, Wood RJ, Majidi C. 2018. Untethered soft robotics. *Nat. Electron.* 1:102–12
9. Hines L, Petersen K, Lum GZ, Sitti M. 2017. Soft actuators for small-scale robotics. *Adv. Mater.* 29:1603483
10. Cianchetti M, Laschi C, Menciassi A, Dario P. 2018. Biomedical applications of soft robotics. *Nat. Rev. Mater.* 3:143–53
11. Banerjee H, Tsz Z, Tse H, Ren H. 2018. Soft robotics with compliance and adaptation for biomedical applications and forthcoming challenges. *Int. J. Robot. Autom.* 33. **https://doi.org/10.2316/journal.206.2018.1.206-4981**
12. O'Neill CT, Phipps NS, Cappello L, Paganoni S, Walsh CJ. 2017. A soft wearable robot for the shoulder: design, characterization, and preliminary testing. In *2017 International Conference on Rehabilitation Robotics*, pp. 1672–78. Piscataway, NJ: IEEE
13. Chen B, Zhao X. 2017. PVC gel soft actuator-based wearable assist wear for hip joint support during walking. *Smart Mater. Struct.* 26:125003
14. Cui H, Zhao Q, Wang Y, Du X. 2019. Bioinspired actuators based on stimuli-responsive polymers. *Chem. Asian J.* 14:2369–87

15. Yang GZ, Bellingham J, Dupont PE, Fischer P, Floridi L, et al. 2018. The grand challenges of science robotics. *Sci. Robot.* 3:eaar7650
16. Jang KI, Chung HU, Xu S, Lee CH, Luan H, et al. 2015. Soft network composite materials with deterministic and bio-inspired designs. *Nat. Commun.* 6:6566
17. Wirekoh J, Park Y. 2017. Design of flat pneumatic artificial muscles. *Smart Mater. Struct.* 26:035009
18. Truby RL, Wehner M, Grosskopf AK, Vogt DM, Uzel SGM, et al. 2018. Soft somatosensitive actuators via embedded 3D printing. *Adv. Mater.* 30:1706383
19. Fras J, Noh Y, Wurdemann H, Althoefer K. 2017. Soft fluidic rotary actuator with improved actuation properties. In *2017 IEEE/RSJ International Conference on Intelligent Robots and Systems*, pp. 5610–15. Piscataway, NJ: IEEE
20. Wang H, Totaro M, Beccai L. 2018. Toward perceptive soft robots: progress and challenges. *Adv. Sci.* 5:1800541
21. Zhao H, Huang R, Shepherd RF. 2016. Curvature control of soft orthotics via low cost solid-state optics. In *2016 IEEE International Conference on Robotics and Automation*, pp. 4008–13. Piscataway, NJ: IEEE
22. Miriyev A, Stack K, Lipson H. 2017. Soft material for soft actuators. *Nat. Commun.* 8:596
23. Tolley MT, Shepherd RF, Karpelson M, Bartlett NW, Galloway KC, et al. 2014. An untethered jumping soft robot. In *2014 IEEE/RSJ International Conference on Intelligent Robots and Systems*, pp. 561–66. Piscataway, NJ: IEEE
24. Nawroth JC, Lee H, Feinberg AW, Ripplinger CM, McCain ML, et al. 2012. A tissue-engineered jellyfish with biomimetic propulsion. *Nat. Biotechnol.* 30:792–97
25. Park SJ, Gazzola M, Park KS, Park S, Di Santo V, et al. 2016. Phototactic guidance of a tissue-engineered soft-robotic ray. *Science* 353:158–62
26. He Q, Wang Z, Wang Y, Song Z, Cai S. 2020. Recyclable and self-repairable fluid-driven liquid crystal elastomer actuator. *ACS Appl. Mater. Interfaces* 12:35464–74
27. Zeng H, Wasylczyk P, Wiersma DS, Priimagi A. 2018. Light robots: bridging the gap between microrobotics and photomechanics in soft materials. *Adv. Mater.* 30:1703554
28. Kim SJ, Kim MS, Kim SI, Spinks GM, Kim BC, Wallace GG. 2006. Self-oscillatory actuation at constant DC voltage with pH-sensitive chitosan/polyaniline hydrogel blend. *Chem. Mater.* 18:5805–9
29. Shin B, Ha J, Lee M, Park K, Park GH, et al. 2018. Hygrobot: a self-locomotive ratcheted actuator powered by environmental humidity. *Sci. Robot.* 3:eaar2629
30. Bira N, Dhagat P, Davidson JR. 2020. A review of magnetic elastomers and their role in soft robotics. *Front. Robot. AI* 7:588391
31. Wu Y, Yim JK, Liang J, Shao Z, Qi M, et al. 2019. Insect-scale fast moving and ultrarobust soft robot. *Sci. Robot.* 4:eaax1594
32. Ikeda T, Mamiya JI, Yu Y. 2007. Photomechanics of liquid-crystalline elastomers and other polymers. *Angew. Chem. Int. Ed.* 46:506–28
33. He Q, Wang Z, Song Z, Cai S. 2019. Bioinspired design of vascular artificial muscle. *Adv. Mater. Technol.* 4:1800244
34. Yu Y, Nakano M, Ikeda T. 2003. Directed bending of a polymer film by light. *Nature* 425:145
35. White TJ, Broer DJ. 2015. Programmable and adaptive mechanics with liquid crystal polymer networks and elastomers. *Nat. Mater.* 14:1087–98
36. Wang C, Sim K, Chen J, Kim H, Rao Z, et al. 2018. Soft ultrathin electronics innervated adaptive fully soft robots. *Adv. Mater.* 30:1706695
37. Kurihara S, Ikeda T, Tazuke S, Seto JE. 1991. Isothermal phase transition of liquid crystals induced by photoisomerization of doped spiropyrans. *J. Chem. Soc. Faraday Trans.* 87:3251–54
38. Allinson H, Gleeson HF. 1993. Physical properties of mixtures of low molar mass nematic liquid crystals with photochromic fulgide guest dyes. *Liq. Cryst.* 14:1469–78
39. White TJ, Serak SV, Tabiryan NV, Vaia RA, Bunning TJ. 2009. Polarization-controlled, photodriven bending in monodomain liquid crystal elastomer cantilevers. *J. Mater. Chem.* 19:1080–85
40. Wang Z, Li K, He Q, Cai S. 2019. A light-powered ultralight tensegrity robot with high deformability and load capacity. *Adv. Mater.* 31:1806849
41. Ahn C, Liang X, Cai S. 2019. Bioinspired design of light-powered crawling, squeezing, and jumping untethered soft robot. *Adv. Mater. Technol.* 4:1900185

42. Tian H, Wang Z, Chen Y, Shao J, Gao T, Cai S. 2018. Polydopamine-coated main-chain liquid crystal elastomer as optically driven artificial muscle. *ACS Appl. Mater. Interfaces* 10:8307–16
43. Liu X, Wei R, Hoang PT, Wang X, Liu T, Keller P. 2015. Reversible and rapid laser actuation of liquid crystalline elastomer micropillars with inclusion of gold nanoparticles. *Adv. Funct. Mater.* 25:3022–32
44. Spillmann CM, Naciri J, Ratna BR, Selinger RLB, Selinger JV. 2016. Electrically induced twist in smectic liquid-crystalline elastomers. *J. Phys. Chem. B* 120:636–72
45. Yuan C, Roach DJ, Dunn CK, Mu Q, Kuang X, et al. 2017. 3D printed reversible shape changing soft actuators assisted by liquid crystal elastomers. *Soft Matter* 13:5558–68
46. Ding M, Jing L, Yang H, Machnicki CE, Fu X, et al. 2020. Multifunctional soft machines based on stimuli-responsive hydrogels: from freestanding hydrogels to smart integrated systems. *Mater. Today Adv.* 8:100088
47. Jeon SJ, Hauser AW, Hayward RC. 2017. Shape-morphing materials from stimuli-responsive hydrogel hybrids. *Acc. Chem. Res.* 50:161–69
48. Paley DA, Wereley NM, eds. 2021. *Bioinspired Sensing, Actuation, and Control in Underwater Soft Robotic Systems.* Cham, Switz.: Springer
49. Taylor M, Tomlins P, Sahota T. 2017. Thermoresponsive gels. *Gels* 3:4
50. Xia LW, Xie R, Ju XJ, Wang W, Chen Q, Chu LY. 2013. Nano-structured smart hydrogels with rapid response and high elasticity. *Nat. Commun.* 4:2226
51. Kim YS, Liu M, Ishida Y, Ebina Y, Osada M, et al. 2015. Thermoresponsive actuation enabled by permittivity switching in an electrostatically anisotropic hydrogel. *Nat. Mater.* 14:1002–7
52. Hua M, Wu D, Wu S, Ma Y, Alsaid Y, He X. 2020. 4D printable tough and thermoresponsive hydrogels. *ACS Appl. Mater. Interfaces* 13:12689–97
53. Li C, Iscen A, Sai H, Sato K, Sather NA, et al. 2020. Supramolecular-covalent hybrid polymers for light-activated mechanical actuation. *Nat. Mater.* 19:900–9
54. Haq MA, Su Y, Wang D. 2017. Mechanical properties of PNIPAM based hydrogels: a review. *Mater. Sci. Eng. C* 70:842–55
55. Zhang JT, Cheng SX, Huang SW, Zhuo RX. 2003. Temperature-sensitive poly (*N*-isopropylacrylamide) hydrogels with macroporous structure and fast response rate. *Macromol. Rapid Commun.* 24:447–51
56. Deng Z, Guo Y, Ma PX, Guo B. 2018. Rapid thermal responsive conductive hybrid cryogels with shape memory properties, photothermal properties and pressure dependent conductivity. *J. Colloid Interface Sci.* 526:281–94
57. Qian X, Zhao Y, Alsaid Y, Wang X, Hua M, et al. 2019. Artificial phototropism for omnidirectional tracking and harvesting of light. *Nat. Nanotechnol.* 14:1048–55
58. Haraguchi K. 2007. Nanocomposite hydrogels. *Curr. Opin. Solid State Mater. Sci.* 11:47–54
59. Hua M, Wu S, Ma Y, Zhao Y, Chen Z, et al. 2021. Strong tough hydrogels via the synergy of freeze-casting and salting out. *Nature* 590:594–99
60. Wu S, Hua M, Alsaid Y, Du Y, Ma Y, et al. 2021. Poly(vinyl alcohol) hydrogels with broad-range tunable mechanical properties via the Hofmeister effect. *Adv. Mater.* 33:2007829
61. Zhang JT, Bhat R, Jandt KD. 2009. Temperature-sensitive PVA/PNIPAAm semi-IPN hydrogels with enhanced responsive properties. *Acta Biomater.* 5:488–97
62. Zhang KY, Liu S, Zhao Q, Huang W. 2016. Stimuli-responsive metallopolymers. *Coord. Chem. Rev.* 319:180–95
63. Takashima Y, Hatanaka S, Otsubo M, Nakahata M, Kakuta T, et al. 2012. Expansion–contraction of photoresponsive artificial muscle regulated by host-guest interactions. *Nat. Commun.* 3:1270
64. Satoh T, Sumaru K, Takagi T, Kanamori T. 2011. Fast-reversible light-driven hydrogels consisting of spirobenzopyran-functionalized poly(*N*-isopropylacrylamide). *Soft Matter* 7:8030–34
65. Ma C, Le X, Tang X, He J, Xiao P, et al. 2016. A multiresponsive anisotropic hydrogel with macroscopic 3D complex deformations. *Adv. Funct. Mater.* 26:8670–76
66. Zhang X, Pint CL, Lee MH, Schubert BE, Jamshidi A, et al. 2011. Optically- and thermally-responsive programmable materials based on carbon nanotube-hydrogel polymer composites. *Nano Lett.* 11:3239–44
67. Yoon C, Xiao R, Park J, Cha J, Nguyen TD, Gracias DH. 2014. Functional stimuli responsive hydrogel devices by self-folding. *Smart Mater. Struct.* 23:094008

68. Ma Y, Hua M, Wu S, Du Y, Pei X, et al. 2020. Bioinspired high-power-density strong contractile hydrogel by programmable elastic recoil. *Sci. Adv.* 6:eabd2520
69. Yuk H, Lin S, Ma C, Takaffoli M, Fang NX, Zhao X. 2017. Hydraulic hydrogel actuators and robots optically and sonically camouflaged in water. *Nat. Commun.* 8:14230
70. Calvert P. 2009. Hydrogels for soft machines. *Adv. Mater.* 21:743–56
71. Khodambashi R, Alsaid Y, Rico R, Marvi H, Peet MM, et al. 2021. Heterogeneous hydrogel structures with spatiotemporal reconfigurability using addressable and tunable voxels. *Adv. Mater.* 33:2005906
72. Alsaid Y, Wu S, Wu D, Du Y, Shi L, et al. 2021. Tunable sponge-like hierarchically porous hydrogels with simultaneously enhanced diffusivity and mechanical properties. *Adv. Mater.* 33:2008235
73. Yuk H, Lin S, Ma C, Takaffoli M, Fang NX, Zhao X. 2017. Hydraulic hydrogel actuators and robots optically and sonically camouflaged in water. *Nat. Commun.* 8:14230
74. Zheng SY, Shen Y, Zhu F, Yin J, Qian J, Fu J. 2018. Programmed deformations of 3D-printed tough physical hydrogels with high response speed and large output force. *Adv. Funct. Mater.* 28:1803366
75. Yang C, Cheng S, Yao X, Nian G, Liu Q, Suo Z. 2020. Ionotronic luminescent fibers, fabrics, and other configurations. *Adv. Mater.* 32:2005545
76. Chung T, Romo-Uribe A, Mather PT. 2008. Two-way reversible shape memory in a semicrystalline network. *Macromolecules* 41:184–92
77. Li J, Rodgers WR, Xie T. 2011. Semi-crystalline two-way shape memory elastomer. *Polymer* 52:5320–25
78. Gao Y, Liu W, Zhu S. 2017. Polyolefin thermoplastics for multiple shape and reversible shape memory. *ACS Appl. Mater. Interfaces* 9:4882–89
79. Hu W, Lum GZ, Mastrangeli M, Sitti M. 2018. Small-scale soft-bodied robot with multimodal locomotion. *Nature* 554:81–85
80. Amjadi M, Sitti M. 2018. Self-sensing paper actuators based on graphite-carbon nanotube hybrid films. *Adv. Sci.* 5:1800239
81. Gao Y, Liu W, Zhu S. 2018. Reversible shape memory polymer from semicrystalline poly(ethylene-co-vinyl acetate) with dynamic covalent polymer networks. *Macromolecules* 51:8956–63
82. Behl M, Kratz K, Zotzmann J, Nöchel U, Lendlein A. 2013. Reversible bidirectional shape-memory polymers. *Adv. Mater.* 25:4466–69
83. Ge F, Lu X, Xiang J, Tong X, Zhao Y. 2017. An optical actuator based on gold-nanoparticle-containing temperature-memory semicrystalline polymers. *Angew. Chem. Int. Ed.* 56:6126–30
84. Wang K, Zhu XX. 2018. Two-way reversible shape memory polymers containing polydopamine nanospheres: light actuation, robotic locomotion, and artificial muscles. *ACS Biomater. Sci. Eng.* 4:3099–106
85. Wang X, Sparkman J, Gou J. 2017. Electrical actuation and shape memory behavior of polyurethane composites incorporated with printed carbon nanotube layers. *Compos. Sci. Technol.* 141:8–15
86. Zhang F, Xia Y, Wang L, Liu L, Liu Y, Leng J. 2018. Conductive shape memory microfiber membranes with core-shell structures and electroactive performance. *ACS Appl. Mater. Interfaces* 10:35526–32
87. Joyee EB, Pan Y. 2019. A fully three-dimensional printed inchworm-inspired soft robot with magnetic actuation. *Soft Robot.* 6:333–45
88. Almansouri AS, Alsharif NA, Khan MA, Swanepoel L, Kaidarova A, et al. 2019. An imperceptible magnetic skin. *Adv. Mater. Technol.* 4:1900493
89. Tang J, Tong Z, Xia Y, Liu M, Lv Z, et al. 2018. Super tough magnetic hydrogels for remotely triggered shape morphing. *J. Mater. Chem. B* 6:2713–22
90. Maffli L, Rosset S, Ghilardi M, Carpi F, Shea H. 2015. Ultrafast all-polymer electrically tunable silicone lenses. *Adv. Funct. Mater.* 25:1656–65
91. Shintake J, Rosset S, Schubert B, Floreano D, Shea H. 2016. Versatile soft grippers with intrinsic electroadhesion based on multifunctional polymer actuators. *Adv. Mater.* 28:231–38
92. Ji X, Liu X, Cacucciolo V, Imboden M, Civet Y, et al. 2019. An autonomous untethered fast soft robotic insect driven by low-voltage dielectric elastomer actuators. *Sci. Robot.* 4:eaaz6451
93. Poulin A, Rosset S, Shea HR. 2015. Printing low-voltage dielectric elastomer actuators. *Appl. Phys. Lett.* 107:244104

94. Niu X, Stoyanov H, Hu W, Leo R, Brochu P, Pei Q. 2013. Synthesizing a new dielectric elastomer exhibiting large actuation strain and suppressed electromechanical instability without prestretching. *J. Polym. Sci. B* 51:197–206
95. Risse S, Kussmaul B, Krüger H, Kofod G. 2012. Synergistic improvement of actuation properties with compatibilized high permittivity filler. *Adv. Funct. Mater.* 22:3958–62
96. Dünki SJ, Ko YS, Nüesch FA, Opris DM. 2015. Self-repairable, high permittivity dielectric elastomers with large actuation strains at low electric fields. *Adv. Funct. Mater.* 25:2467–75
97. Rothemund P, Kellaris N, Mitchell SK, Acome E, Keplinger C. 2020. HASEL artificial muscles for a new generation of lifelike robots—recent progress and future opportunities. *Adv. Mater.* 33:2003375
98. Li T, Zou Z, Mao G, Yang X, Liang Y, et al. 2019. Agile and resilient insect-scale robot. *Soft Robot.* 6:133–41
99. Li T, Li G, Liang Y, Cheng T, Dai J, et al. 2017. Fast-moving soft electronic fish. *Sci. Adv.* 3:e1602045
100. Chen Y, Zhao H, Mao J, Chirarattananon P, Helbling EF, et al. 2019. Controlled flight of a microrobot powered by soft artificial muscles. *Nature* 575:324–29
101. Kruusamäe K, Punning A, Aabloo A, Asaka K. 2015. Self-sensing ionic polymer actuators: a review. *Actuators* 4:17–38
102. Madden JD, Cush RA, Kanigan TS, Hunter I. 2000. Fast contracting polypyrrole actuators. *Synth. Met.* 133:185–92
103. Hu F, Xue Y, Xu J, Lu B. 2019. PEDOT-based conducting polymer actuators. *Front. Robot. AI* 6:114
104. Melling D, Martinez JG, Jager EWH. 2019. Conjugated polymer actuators and devices: progress and opportunities. *Adv. Mater.* 31:1808210
105. Otero TF, Martinez JG. 2015. Physical and chemical awareness from sensing polymeric artificial muscles. Experiments and modeling. *Prog. Polym. Sci.* 44:62–78
106. Yang M, Yuan Z, Liu J, Fang Z, Fang L, et al. 2019. Photoresponsive actuators built from carbon-based soft materials. *Adv. Opt. Mater.* 7:1900069
107. Kim H, Lee H, Ha I, Jung J, Won P, et al. 2018. Biomimetic color changing anisotropic soft actuators with integrated metal nanowire percolation network transparent heaters for soft robotics. *Adv. Funct. Mater.* 28:1801847
108. Yoon CK. 2019. Advances in biomimetic stimuli responsive soft grippers. *Nano Converg.* 6:20
109. Wani OM, Zeng H, Priimagi A. 2017. A light-driven artificial flytrap. *Nat. Commun.* 8:15546
110. Gladman AS, Matsumoto EA, Nuzzo RG, Mahadevan L, Lewis JA. 2016. Biomimetic 4D printing. *Nat. Mater.* 15:413–18
111. Zhuo S, Zhao Z, Xie Z, Hao Y, Xu Y, et al. 2020. Complex multiphase organohydrogels with programmable mechanics toward adaptive soft-matter machines. *Sci. Adv.* 6:eaax1464
112. Tian H, Liu H, Shao J, Li S, Li X, Chen X. 2020. An electrically active gecko-effect soft gripper under a low voltage by mimicking gecko's adhesive structures and toe muscles. *Soft Matter* 16:5599–5608
113. Fang X, Liu Z, Hao Y, Yang H, Liu J, et al. 2019. A soft actuator with tunable mechanical configurations for object grasping based on sensory feedback. In *2019 2nd IEEE International Conference on Soft Robotics*, pp. 25–30. Piscataway, NJ: IEEE
114. Zeng H, Wani OM, Wasylczyk P, Kaczmarek R, Priimagi A. 2017. Self-regulating iris based on light-actuated liquid crystal elastomer. *Adv. Mater.* 29:1701814
115. Wani OM, Zeng H, Wasylczyk P, Priimagi A. 2018. Programming photoresponse in liquid crystal polymer actuators with laser projector. *Adv. Opt. Mater.* 6:1700949
116. Jung K, Koo JC, Nam J, Lee YK, Choi HR. 2007. Artificial annelid robot driven by soft actuators. *Bioinspir. Biomim.* 2:S42
117. Menciassi A, Gorini S, Pernorio G, Liu W, Valvo F, Dario P. 2004. Design, fabrication and performances of a biomimetic robotic earthworm. In *2004 IEEE International Conference on Robotics and Biomimetics*, pp. 274–78. Piscataway, NJ: IEEE
118. Rogóż M, Zeng H, Xuan C, Wiersma DS, Wasylczyk P. 2016. Light-driven soft robot mimics caterpillar locomotion in natural scale. *Adv. Opt. Mater.* 4:1689–94
119. Gelebart AH, Mulder DJ, Varga M, Konya A, Vantomme G, et al. 2017. Making waves in a photoactive polymer film. *Nature* 546:632–36

120. Lu X, Guo S, Tong X, Xia H, Zhao Y. 2017. Tunable photocontrolled motions using stored strain energy in malleable azobenzene liquid crystalline polymer actuators. *Adv. Mater.* 29:1606467
121. Hu Y, Liu J, Chang L, Yang L, Xu A, et al. 2017. Electrically and sunlight-driven actuator with versatile biomimetic motions based on rolled carbon nanotube bilayer composite. *Adv. Funct. Mater.* 27:1704388
122. Zeng H, Wasylczyk P, Parmeggiani C, Martella D, Burresi M, Wiersma DS. 2015. Light-fueled microscopic walkers. *Adv. Mater.* 27:3883–87
123. Zeng H, Wani OM, Wasylczyk P, Priimagi A. 2018. Light-driven, caterpillar-inspired miniature inching robot. *Macromol. Rapid Commun.* 39:1700224
124. Wie JJ, Shankar MR, White TJ. 2016. Photomotility of polymers. *Nat. Commun.* 7:13260
125. Purcell EM. 1977. Life at low Reynolds number. *Am. J. Phys.* 45:3–11
126. Zhang H, Mourran A, Möller M. 2017. Dynamic switching of helical microgel ribbons. *Nano Lett.* 17:2010–14
127. Mourran A, Zhang H, Vinokur R, Möller M. 2017. Soft microrobots employing nonequilibrium actuation via plasmonic heating. *Adv. Mater.* 29:1604825
128. Palagi S, Mark AG, Reigh SY, Melde K, Qiu T, et al. 2016. Structured light enables biomimetic swimming and versatile locomotion of photoresponsive soft microrobots. *Nat. Mater.* 15:647–53
129. Diller E, Zhuang J, Zhan Lum G, Edwards MR, Sitti M. 2014. Continuously distributed magnetization profile for millimeter-scale elastomeric undulatory swimming. *Appl. Phys. Lett.* 104:174101
130. Huang C, Lv JA, Tian X, Wang Y, Yu Y, Liu J. 2015. Miniaturized swimming soft robot with complex movement actuated and controlled by remote light signals. *Sci. Rep.* 5:17414
131. Zhang L, Abbott JJ, Dong L, Kratochvil BE, Bell D, Nelson BJ. 2009. Artificial bacterial flagella: fabrication and magnetic control. *Appl. Phys. Lett.* 94:2007–10
132. Kim B, Kim D, Jung J. 2005. A biomimetic undulatory tadpole robot using ionic polymer–metal composite. *Smart Mater. Struct.* 14:1579
133. Tan X, Kim D, Usher N, Laboy D, Jackson J, et al. 2006. An autonomous robotic fish for mobile sensing. In *2006 IEEE/RSJ International Conference on Intelligent Robots and Systems*, pp. 5424–29. Piscataway, NJ: IEEE
134. Gu H, Boehler Q, Cui H, Secchi E, Savorana G, et al. 2020. Magnetic cilia carpets with programmable metachronal waves. *Nat. Commun.* 11:2637
135. Gelebart AH, Vantomme G, Meijer EW, Broer DJ. 2017. Mastering the photothermal effect in liquid crystal networks: a general approach for self-sustained mechanical oscillators. *Adv. Mater.* 29:1606712
136. Serak S, Tabiryan N, Vergara R, White TJ, Vaia RA, Bunning TJ. 2010. Liquid crystalline polymer cantilever oscillators fueled by light. *Soft Matter* 6:779–83
137. Yang L, Chang L, Hu Y, Huang M, Ji Q, et al. 2020. An autonomous soft actuator with light-driven self-sustained wavelike oscillation for phototactic self-locomotion and power generation. *Adv. Funct. Mater.* 30:1908842
138. White TJ, Tabiryan NV, Serak SV, Hrozhyk UA, Tondiglia VP, et al. 2008. A high frequency photodriven polymer oscillator. *Soft Matter* 4:1796
139. Lee KM, Smith ML, Koerner H, Tabiryan N, Vaia RA, et al. 2011. Photodriven, flexural-torsional oscillation of glassy azobenzene liquid crystal polymer networks. *Adv. Funct. Mater.* 21:2913–18
140. Kumar K, Knie C, Bléger D, Peletier MA, Friedrich H, et al. 2016. A chaotic self-oscillating sunlight-driven polymer actuator. *Nat. Commun.* 7:11975
141. Wang XQ, Tan CF, Chan KH, Lu X, Zhu L, et al. 2018. In-built thermo-mechanical cooperative feedback mechanism for self-propelled multimodal locomotion and electricity generation. *Nat. Commun.* 9:3438
142. Chen Y, Wang H, Helbling EF, Jafferis NT, Zufferey R, et al. 2017. A biologically inspired, flapping-wing, hybrid aerial-aquatic microrobot. *Sci. Robot.* 2:eaao5619
143. Ma KY, Chirarattananon P, Fuller SB, Wood RJ. 2013. Controlled flight of a biologically inspired, insect-scale robot. *Science* 340:603–7
144. Yuan X, Liu H, Zou J, Jin G, Sun L. 2019. Soft tactile sensor and curvature sensor for caterpillar-like soft robot's adaptive motion. In *RICAI 2019: Proceedings of the 2019 International Conference on Robotics, Intelligent Control and Artificial Intelligence*, pp. 690–95. New York: ACM

145. Zhao H, O'Brien K, Li S, Shepherd RF. 2016. Optoelectronically innervated soft prosthetic hand via stretchable optical waveguides. *Sci. Robot.* 1:eaai7529
146. Zhao Y, Lo C-Y, Ruan L, Pi C-H, Kim C, et al. 2021. Somatosensory actuator based on stretchable conductive photothermally responsive hydrogel. *Sci. Robot.* 6:eabd5483
147. Larson C, Peele B, Li S, Robinson S, Totaro M, et al. 2016. Highly stretchable electroluminescent skin for optical signaling and tactile sensing. *Science* 351:1071–74
148. Cheng H, Zhao F, Xue J, Shi G, Jiang L, Qu L. 2016. One single graphene oxide film for responsive actuation. *ACS Nano* 10:9529–35
149. Wang XQ, Chan KH, Cheng Y, Ding T, Li T, et al. 2020. Somatosensory, light-driven, thin-film robots capable of integrated perception and motility. *Adv. Mater.* 32:2000351
150. Li S, Bai H, Liu Z, Zhang X, Huang C, et al. 2021. Digital light processing of liquid crystal elastomers for self-sensing artificial muscles. *Sci. Adv.* 7:eabg3677

Annual Review of Control, Robotics, and Autonomous Systems

Volume 5, 2022

Contents

Errata

An online log of corrections to *Annual Review of Control, Robotics, and Autonomous Systems* articles may be found at http://www.annualreviews.org/errata/control